IAEA-182

EXPERIMENTAL ASPECTS OF LASER AND ELECTRON-BEAM PRODUCED THERMONUCLEAR PLASMAS

PROCEEDINGS OF AN ADVISORY GROUP MEETING
ON EXPERIMENTAL ASPECTS OF LASER AND
ELECTRON-BEAM PRODUCED THERMONUCLEAR PLASMAS
HELD AT TRIESTE, 25-29 AUGUST 1975
ORGANIZED BY THE
INTERNATIONAL ATOMIC ENERGY AGENCY
TOGETHER WITH THE
INTERNATIONAL CENTRE FOR THEORETICAL PHYSICS, TRIESTE

A TECHNICAL DOCUMENT ISSUED BY THE
INTERNATIONAL ATOMIC ENERGY AGENCY, VIENNA, 1976

PLEASE BE AWARE THAT
ALL OF THE MISSING PAGES IN THIS DOCUMENT
WERE ORIGINALLY BLANK

The IAEA does not maintain stocks of reports in this series. However, microfiche copies of these reports can be obtained from

INIS Microfiche Clearinghouse
International Atomic Energy Agency
Kämtner Ring 11
P.O. Box 590
A-1011 Vienna, Austria

on prepayment of US $0.65 or against one IAEA microfiche service coupon.

FOREWORD

The Advisory Group Meeting on Experimental Aspects of Laser and Electron-Beam Produced Thermonuclear Plasmas was organized by the Agency together with the International Center for Theoretical Physics in Trieste. It was a follow-up of the Workshop on Theoretical Problems of Laser Electron-Beam Plasma Interaction held at the Trieste Center in August 1973. 27 scientists from 10 countries attended the meeting.

In the course of the first two days of the meeting the present state of the art of experiments on laser and electron-beam produced plasmas were reviewed by the representatives of several major laboratories and are included in this publication. Workshop-type sessions on the following selected topics were held:

1. Laser systems
2. Interaction of laser beam with target plasma
3. Laser heating for magnetic confinement
4. Diagnostic of implosion
5. Reactor concepts.

Short résumés of these sessions prepared by the chairmen together with four original papers presented at the meeting are included in this report.

The participants also exchanged their views on the possible role of smaller experiments in the laser and electron-beam fusion programme with the aim to give guidelines to developing countries which would like to start research in this field.

The facilities provided for this meeting by the ICTP were excellent and the Agency would like to acknowledge the personal efforts of Professor Budini and Dr. Hamende of the Center who contributed to the success of the meeting.

Table of Contents

NATIONAL AND LABORATORY REPORTS

Laser Fusion

LASER FUSION RESEARCH IN JAPAN

C. Yamanaka +)

Institute of Laser Engineering, Osaka University, Osaka

Summary:

The following main aims are being pursued in the field of laser fusion research at the Institute of Laser Engineering, Osaka University:

- Development of high power high efficiency lasers
- Study of physics of laser coupling with plasma.
- Development of diagnostics of fine spacial (/um) and temporal (psec) resolution
- Development of technique of a pellet compression.

High power Nd glass laser GEKKO system and E-beam excited CO_2 laser LEKKO system are being developed for these purposes.

GEKKO I - one beam glass laser system with 7 amplifiers, energy output is 50 J in 2 ns, laser beam diameter is 40 mm with a divergence being less than 0.5 m rad, pulse width is adjustable from few tens picoseconds to nanoseconds.

GEKKO II and GEKKO IV are correspondingly two and four-beam systems with an energy of 250 J in each beam.

A twelve-beam glass laser with a total energy of 10 KJ in 0.5 nsec is being planned.

The results achieved with the GEKKO system up to-day are the following:

Parametric decay instability is clarified experimentally. The induced backward Brillouin scattering observed near the second harmonics of the reflected light shows an isotope effect due to the ion acoustic waves in hydrogen and deuterium plasma respectively. A decrease of the reflectivity of the laser light from plasma was ascertained at the laser intensity of ten times larger than the threshold of the parametric decay instability. Spectral broadening due to the self-phase modulation was observed in the backscattered light in the wavelength 1.06 /um. Acceleration mechanisms of fast ion was investigated. A compression experiment is investigated using glass micro balloon filled with D_2 gas.

LEKKO I - is high pressure E-beam CO_2 laser with two stages of TEA laser preamplifier and three-stages CO_2 main amplifier; the output energy is 200 J in one nanosecond. LEKKO III, a two-beam system to deliver 1 KJ in one nanosecond is under construction.

+) Composed from records of oral presentation

The following results have been obtained with the LEKKO system:

Anomalous heating due to parametric instability has been clarified. The threshold laser power intensity for this process is 10^{10} W/cm^2. Below the threshold the expansion is thermal which has a power dependence of $Q^{4/9}$, where Q is the incident laser flux. Above the threshold the expansion is flux-limited which shows a power dependence of $Q^{2/3}$. A control technique of oscillating lines by double-laser cavity with a saturable absorber has been accomplished. The pressure broadening coefficient of the CO_2 laser line is derived from the small signal gain dependence on laser gas pressure using a 15 atmosphere pressure E-beam CO_2 laser.

LASER FUSION RESEARCH AT THE LEBEDEV INSTITUTE OF PHYSICS, USSR ACADEMY OF SCIENCES

V. Gribkov

In Basov's Laboratory of the Lebedev Institute the problem of thermonuclear fusion by laser is seen as consisting of the following:

I. Creation of an optimal <u>laser-target system</u> ensuring a maximum amplification coefficient:

$$k = \frac{E_{th}}{E_{las}}$$

II. Development and preparation of the <u>target</u>. This must ensure high average density in the final cumulation state: $10^2 \div 10^3$ g/cm^3, and have a large initial fuel mass (DT, CDT, Li_2DT): 10^{-2} g.

III. Achievement of a maximum <u>conversion coefficient</u> from laser energy to kinetic energy of the collapsing material:

$$\eta = \frac{E_{kin}}{E_{las}} = \eta \left(R_o, \frac{M_o}{M_{vapor.}} (2\ell), q_{las} \ldots.\right)$$

IV. Creation of such <u>cumulation dynamics</u> that the density and temperature profiles before the beginning of combustion are as follows:

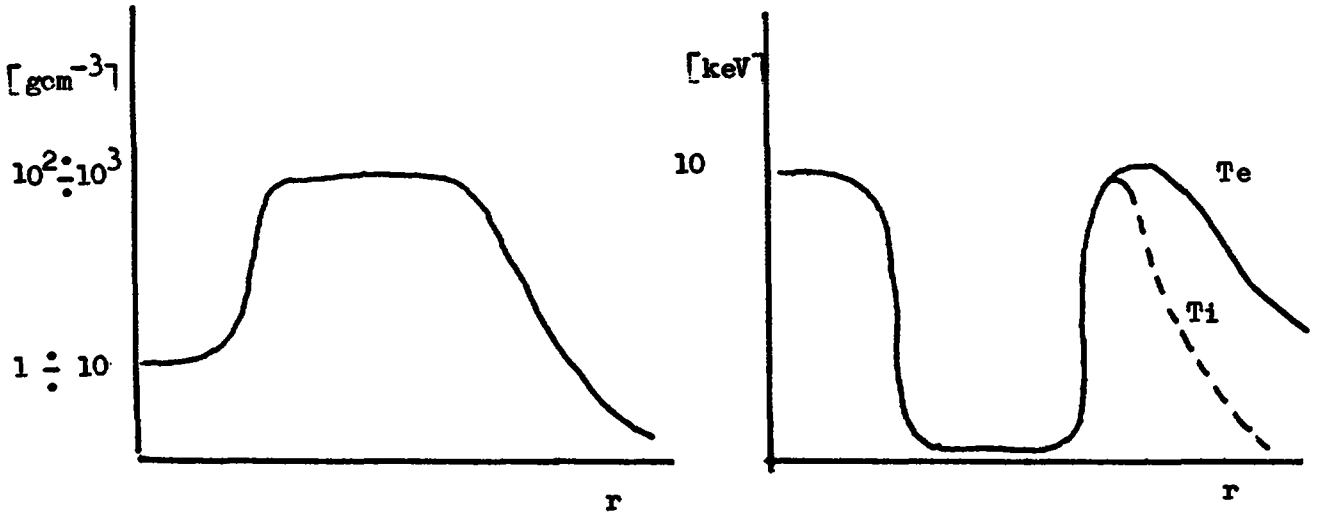

V. Obtaining stability of the compression process.

In N.G. Basov's Laboratory these problems are being solved in the following way:

I. Powerful lasers

(a) On neodymium glass

(1) A 9-channel device has been operating since 1971 ($E = 500$ J, $\tau = 1$ ns, contrast 10^6, $\vartheta = 10^{-3}$ rad)

(2) In 1974 a 20-channel laser device was started up. ($E = 200$ J $\div$ 1 kJ $\div$ 2 kJ; $\tau = 2 \times 10^{-11}$ s $\div$ 10^{-9} s $\div$ 2×10^{-8} s, contrast 10^6, $\vartheta = 3 \times 10^{-4}$ rad)

(3) A 216-channel device is being built which will be started up at the end of 1976, though one quarter will be operating by the end of 1975 ($E = 10$ kJ, $\tau = 1$ ns, luminosity 10^{17} W/cm^2 sterad).

(b) There is an iodine laser operating ($E = 130$ J, $\tau = 1$ ns). Towards the end of 1975 the energy will increase to 500 J.

(c) A high-pressure CO_2-laser is operating ($p = 10^{12}$ W/cm^2).

(d) A chemical laser is being developed ($F_2 + H_2$).

II. In conjunction with Isakov's Laboratory solid and hollow targets have been developed and are being made; they are 50-2000 μm in diameter and consist of hydrogen, polymers, glass and metallic oxides that meet the requirements imposed on targets for laser thermonuclear fusion.

III, IV. (a) In co-operation with the Institute of Applied Mathematics a new type of target has been developed which gives an amplification coefficient $K = 10^2$-10^3 for $E_{las} = 10^4$-10^6 J in a simple (unprofiled) pulse;

(b) In collaboration with Silin's department work is proceeding on the theoretical aspects of the conversion coefficient (absorption, reflection of the laser radiation in the corona, heat conductivity, gas dynamics, etc.);

(c) A number of new methods have been developed for research on laser plasma (interferometry, multichannel X-ray

research, study of reflection, scattering, harmonics generation, DT-neutron diagnostics, X-ray spectroscopy, camera obscura, etc.);

(d) The processes of absorption and harmonics generation, reflection, the distribution function, X-ray anisotropy, etc. have been studied. A 30-fold compression of the target nucleus was achieved;

(e) With the help of the CO_2-laser, experiments on heating are being carried out, plasma density and temperature have been studied and a mode-locking type of working regime with the plasma has been discovered.

V. It has been shown that since the particle lives in the possible instability zone for a very short time (far shorter than the acceleration time), stable working regimes are possible in targets with thin sheaths.

Apart from this, the FLORA device has been set up (together with Isakov's Laboratory and Filippov's Laboratory (of the Kurchatov Institute) and a theory of combined plasma heating with a laser and a relativistic electron beam is being developed (with Silin's department).

In A.M. Prokhorov's Laboratory, in collaboration with Koval'skij, Pergament of the Kurchatov Institute:

I. (a) A 3-channel laser on glass blocks with a rectangular cross-section has been started up (E up to 1 kJ, $\tau = 10^{-10}$–10^{-8} s, $\vartheta = 2 \times 10^{-4}$ rad);

(b) The UMI-35 device is under construction (E = 10 kJ, $\lambda = 1.06$; $0.53\ \mu$). Start-up is planned for the end of 1976 or the beginning of 1977;

(c) Modules are being developed for a CO_2-laser with a planned energy of 1–3 kJ and $\tau = 1$ ns.

III, IV, V. (a) Theoretical work is being done atthe Kurchatov Inst. on complex targets and stability.

(b) Experimental work on absorption, harmonics generation, spontaneous magnetic field measurement, time dependence of X-rays.

(c) New diagnostic methods are being developed: image converters in the visible and X-ray ranges, holograph interferometry, etc.

Thus, further progress lies with the completion of construction of the above-mentioned powerful neodymium, CO_2, iodine and chemical lasers.

LASER FUSION RESEARCH AT LOS ALAMOS

Gene H. McCall

Los Alamos Scientific Laboratory
University of California
Los Alamos, New Mexico 87544
United States of America

Although the progress and current status of laser fusion research can best be described by the results of interaction experiments, these experiments are closely related to the lasers used to produce the plasmas being studied. At Los Alamos the primary emphasis is on CO_2 lasers, but target experiments are being done with both Nd:Glass and CO_2 lasers. The use of both types of laser gives a direct comparison of experiments done at different wavelengths and power. The lasers currently operating and planned are:

Nd:Glass

I. 2-beams 300 GW 100-400 ps pulse
   - A. 80 percent of energy in 250 μrad
   - B. 100 percent of energy in 875 μrad
   - C. Easily extended to 4-beams

II. 1-beam 500 GW 30-50 ps pulse
   - A. Used for diagnostic instrument development

CO_2

I. 1-beam 100 GW 1.5 ns pulse
   - A. Operating for absorption and heating experiments

II. 2-beam ∿ 1 TW 1.5 ns pulse
   - A. Under construction - near completion

III. 8-beam ∿ 10 TW
   - A. Under construction

IV. 6-beam ∿ 100 TW
   - A. Preliminary design

Early Nd:Glass laser target experiments on plane targets at Los Alamos and elsewhere showed that x-ray spectra from these targets could not be described by a single exponential dependence of intensity on photon energy. It was postulated that the electron distribution which produced this spectrum was nonthermal. Calculations done at Livermore showed that the general spectral shape could be produced by a velocity distribution of the form $\exp(-\alpha\ v/v_0)$ where α is an adjustable parameter. It was not possible, however, to reproduce the measured intensity. Recent experiments at the Naval Research Laboratory have confirmed the measurement. Calculations for plasmas generated by a CO_2 laser gave better agreement if a self-generated magnetic field was assumed.

It should be emphasized that these measurements were integrated over both time and space. It is possible, therefore, that the apparent non-Maxwellian electron distribution is only the superposition of Maxwellian distributions, at different temperatures, which exist at different times and at different places in the plasma. Calculations based on this hypothesis have been done by Winsor and Colombant at NRL and by Malone at Los Alamos, and it was found that the data is consistent with this assumption if a mechanism exists for limiting the electron flux from the absorption region to the interior of the plasma. In the NRL calculation a self-consistent magnetic field limited the flux and in the Los Alamos calculation an arbitrary flux limit, which could be due to turbulence, was used.

Figure 1 shows a measurement of the anisotropy of plasma expansion when a thin film of cellulose acetate was used as a target. The data shown are oscilloscope traces from ion time-of-flight detectors located along the normal to the target. The upper trace is from the side of the target toward the laser, and the lower trace is from the detector behind the target. It can be seen that for target thicknesses between 400 Å and 1600 Å the signal does not change much in front, but the ions at the rear are much slower for the thicker target. Calculations based on classical conductivity give an almost

isotropic expansion for the thickest film in this experiment. Thus, a reduction in conductivity is indicated, but Shay at Livermore has shown that the transverse conductivity can reduce the effective intensity by spreading the energy over a region larger than the laser spot size. Even with this effect, however, a flux limit is required to explain the data. In general, the experiments do not distinguish among the models which have been investigated.

A consequence of a hot electron distribution and a cold ion distribution in the absorption region is the electrostatic acceleration of ions by the electric field generated by the hot electrons. Using the description of Morse and Nielson, one finds that the ion energy depends on laser intensity as

$$E_i \sim I^{2/3}$$

Figure 2 shows the measured ion kinetic energy as a function of laser intensity for a polyethylene target illuminated by a CO_2 laser. The $I^{2/3}$ dependence is seen to hold. Another consequence is that the energy per unit charge should be a constant. Figure 3 shows an ion spectrum measured in a Nd:Glass laser experiment which produced a rather cold plasma. The assumption of constant E/Z appears to be justified.

Neutrons can be produced in the corona if ions with sufficient velocity pass through cold material which is ablated early in the laser pulse. If one characterizes the ion expansion by kinetic energy and ion number using the $I^{2/3}$ dependence, it is possible to calculate the neutron yield in these experiments. Figure 4 shows such a calculation for the experiments of Yamanaka and Floux. The agreement is seen to be good over a decade in laser flux and two decades in neutron yield.

Much of the information on the spatial distribution of energy in implosion experiments has been obtained by imaging the soft x-rays emitted by glass microballoon targets. Figure 5 shows the result from this type of experiment. The glass microballoon was mounted on a thin plastic foil and was illuminated by two beams at an intensity of 3×10^{15} W/cm^2. The upper photographs show the data, the center traces are densitometer traces of the photographs, and

the lower figure shows the target. Neutron yields from these targets can be observed from either the "weak" or "strong" implosions.

The interpretation of these photographs is not simple because they are integrated over time and wavelength. To obtain sufficient intensity, x-rays between 1 and 3 keV are used, but most of the radiation is composed of lines and free-bound emission, and a simple interpretation of filtered channels is not possible. Figure 6 is an x-ray spectrum of silicon measured in an experiment in which a 100 μm diameter glass shell was heated by two beams from a Nd:Glass laser. The complicated spectrum clearly shows the free-bound continuum and indicates the need for both spatial and wavelength resolution if one wishes to derive the spatial dependence of electron temperature from these measurements. By placing a narrow slit in front of a KAP crystal spectrometer one can obtain such information. Figure 7 shows such a measurement. The upper densitometer trace shows the spatial dependence of the $1s^2$ - 1s2p resonance line in heliumlike silicon and the lower trace shows the spatial variation of the Lyman-α line in hydrogenlike silicon. Spatial resolution is approximately 50 μm. From the ratio of the lines it can be seen that the center of the shell is at much higher temperature than the outside.

Neutron emission from these targets has been obtained at several laboratories, but, in general, the conditions under which neutrons have been obtained are not relevant for laser fusion. For the small yields which have been obtained (10^6-10^7) the dependence of yield on temperature is much stronger than the dependence on density. In these experiments the DT gas is heated at the expense of density such that compression to the required density for laser fusion would be impossible even if more laser power were available. It should be emphasized that the central problem of laser fusion is the obtaining of high density and not the heating of the fuel. Even in the current experiments, however, it has not been shown that the emitting source is thermal. Only ∿ 1 mJ of ion energy near the

peak energy of the DT reaction cross section would be required to produce the observed yield. Because of the nonthermal processes known to occur in laser-produced plasmas, the possibility of neutron production by these processes should be investigated more carefully. It is not clear, however, that the results would be applicable to experiments which more closely approximate the conditions required for laser fusion. It is suggested, therefore, that more effort be applied to the investigation of processes which occur at density-temperature combinations necessary for laser fusion.

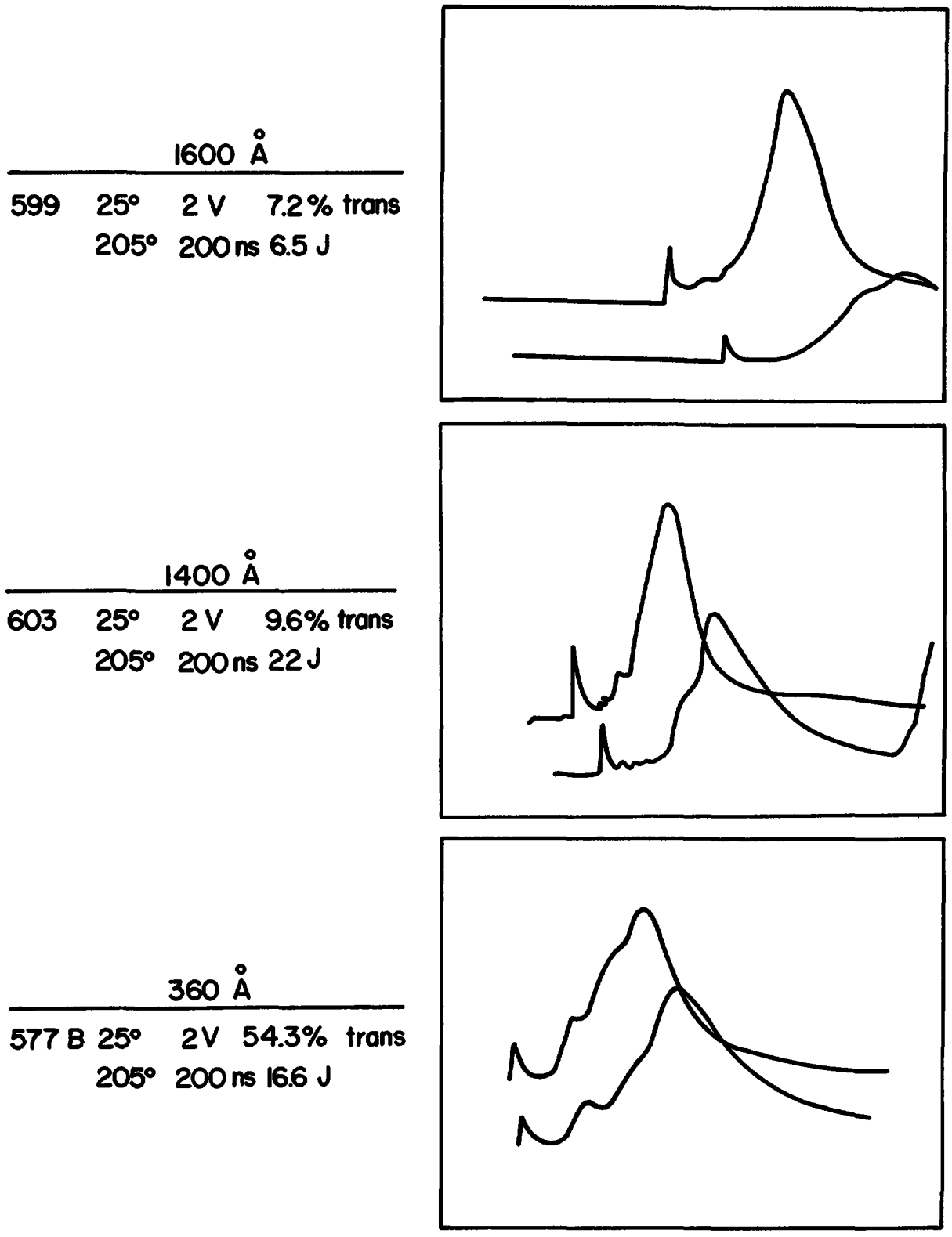

Fig. 1. Ion time-of-flight traces for thin plastic films illuminated by a 30 ps pulse from a Nd:Glass laser. Upper trace is laser side, lower trace is at rear of target. Target thickness in Angstroms.

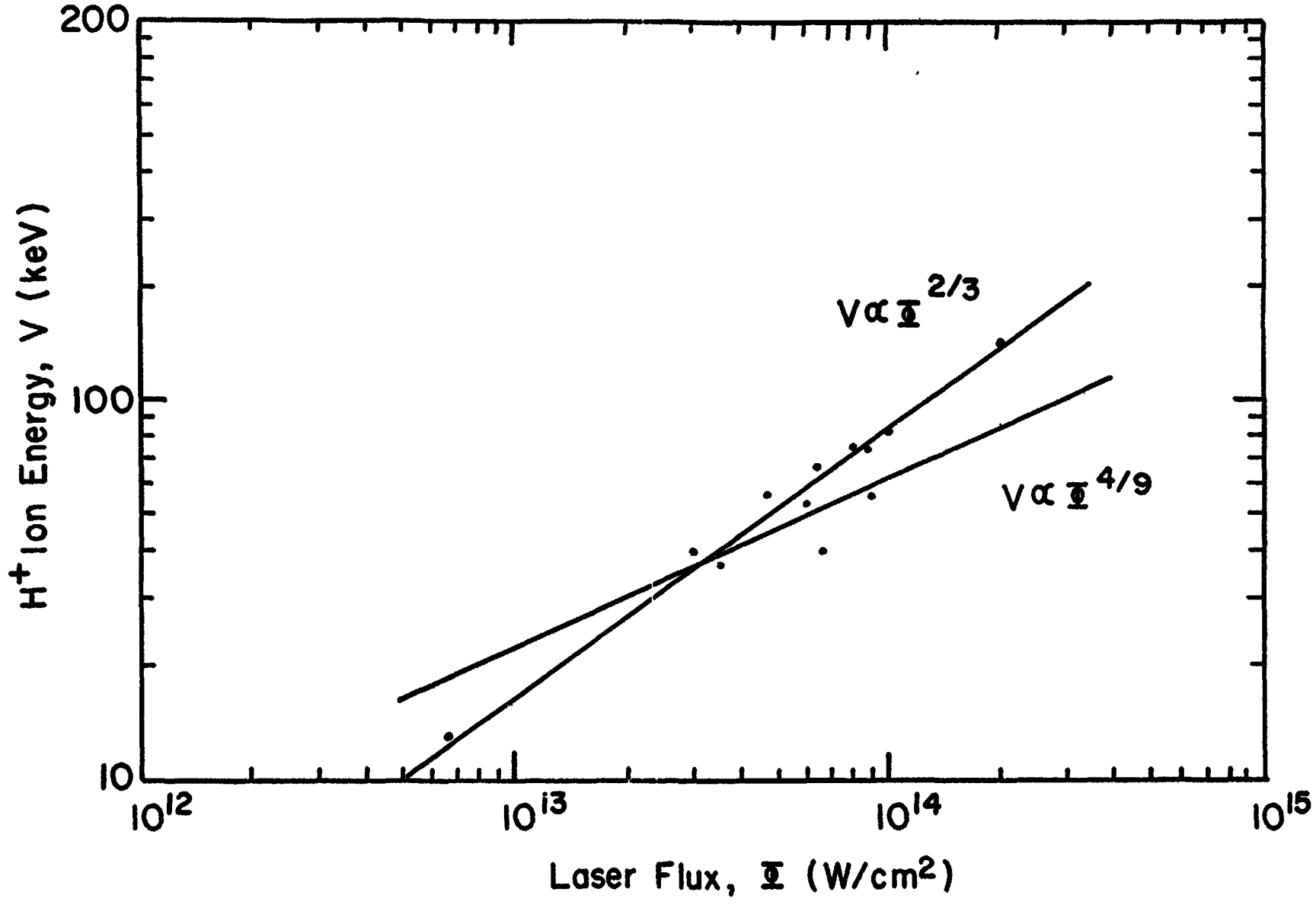

Fig. 2. Kinetic energy of H^+ ions emitted from a CH_2 target illuminated by a CO_2 laser as a function of laser intensity. Pulse width is 1.5 ns.

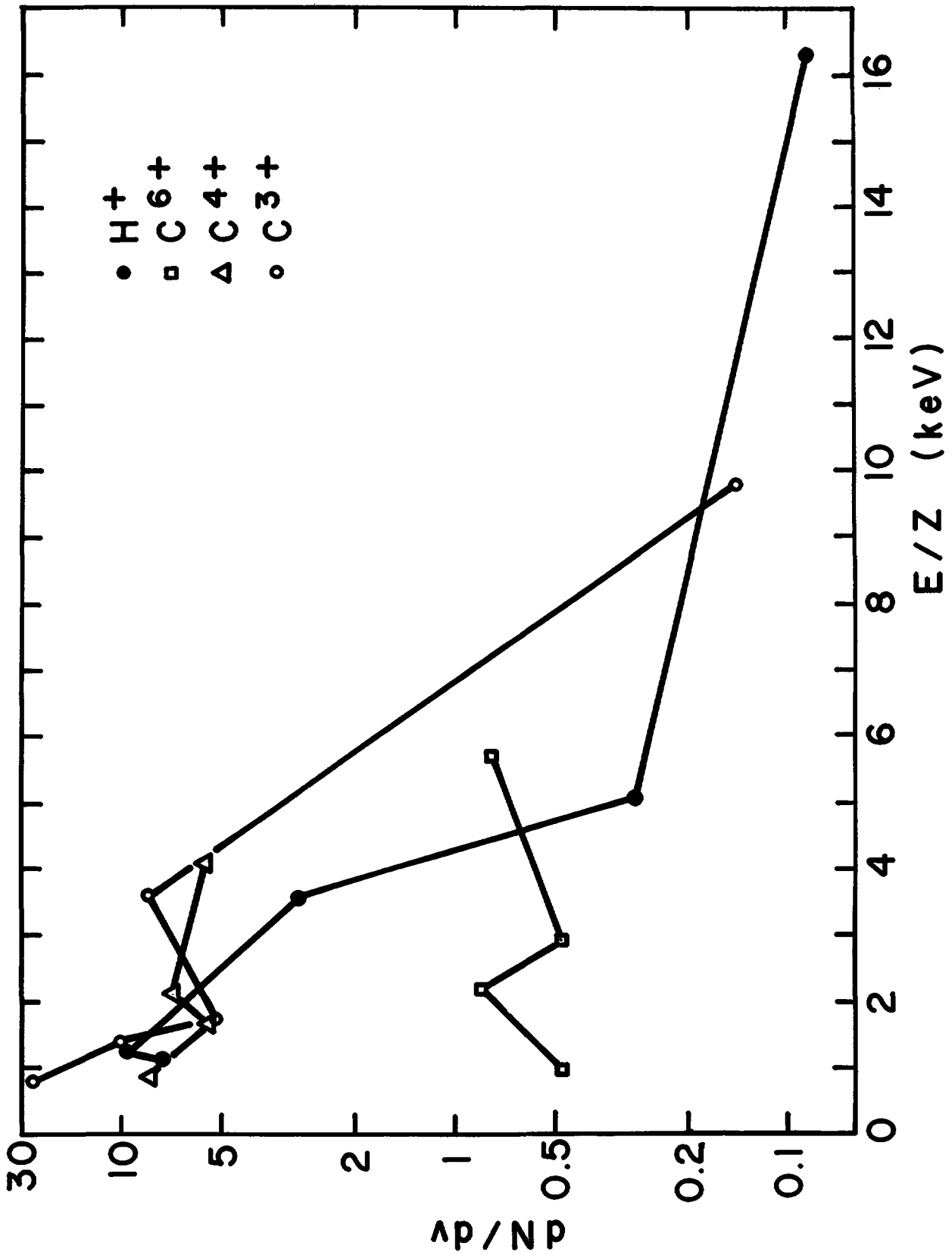

Fig. 3. Ion spectrum from a CH_2 plasma illuminated by a Nd:Glass laser.

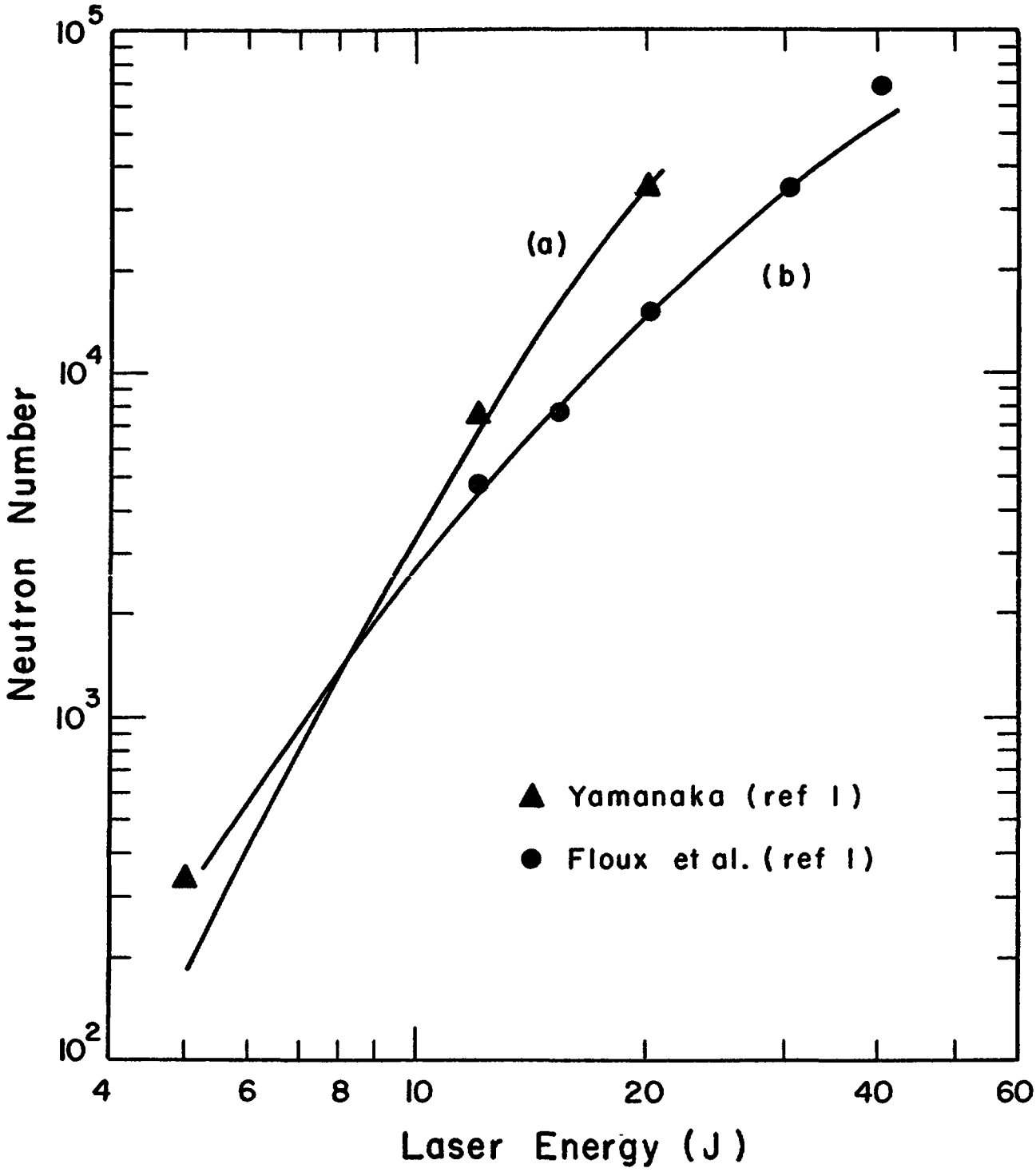

Fig. 4. Comparison of experimental and theoretical results for corona neutrons.

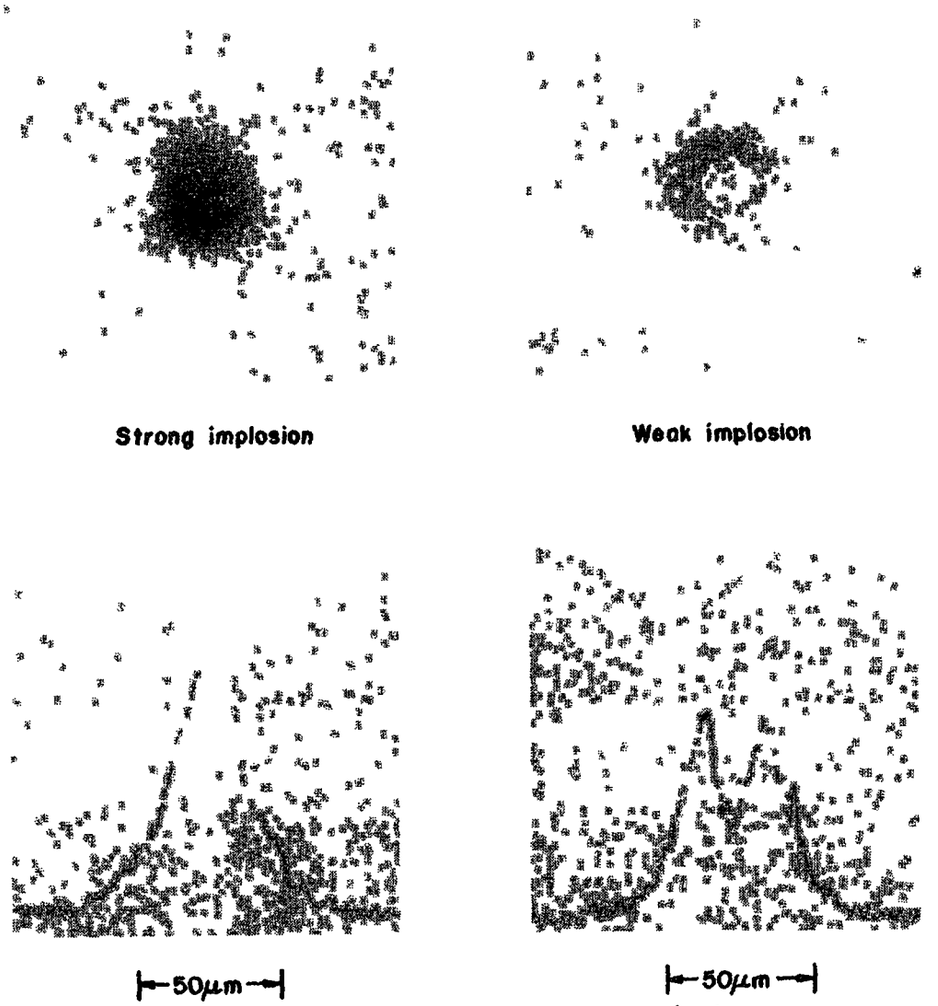

Fig. 5. X-ray pinhole photographs from a glass microballoon illuminated by a two-beam Nd:Glass laser.

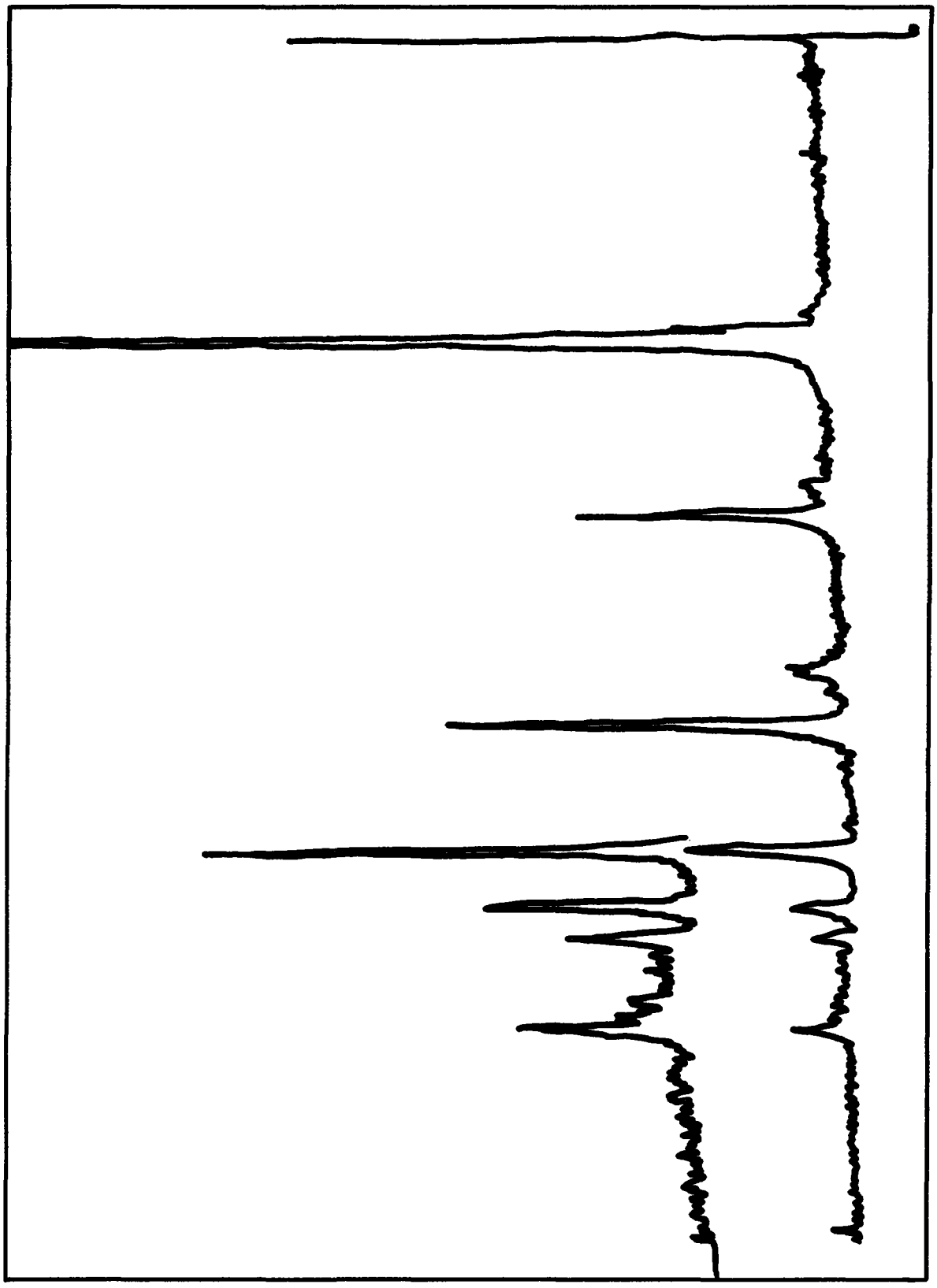

Fig. 6. X-ray spectrum generated by a glass microballoon target. Dispersive element is an EDDT crystal.

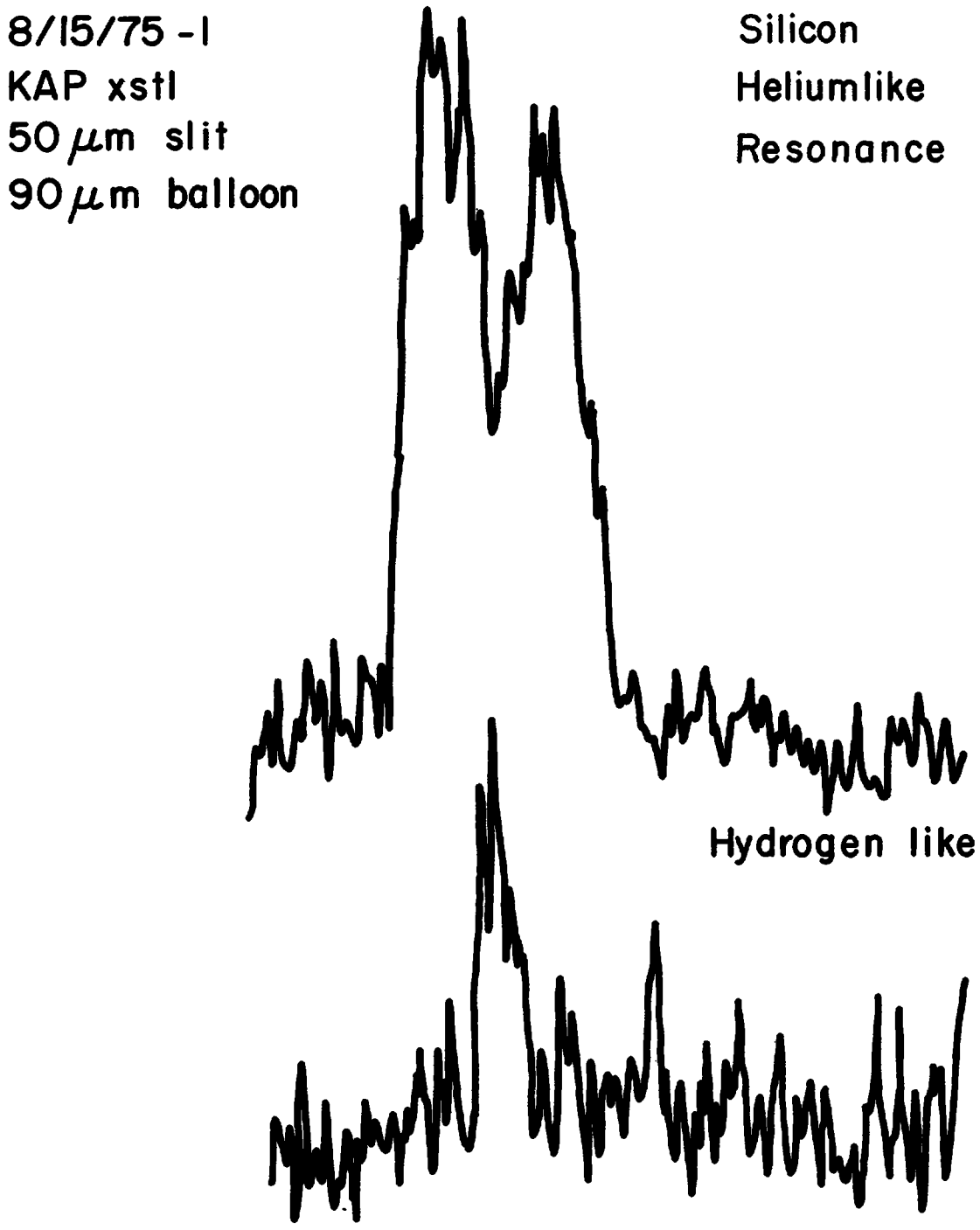

Fig. 7. Spatially resolved x-ray line spectrum of silicon. Spatial resolution is approximately 50 μm.

REVIEW OF ERDA INERTIAL CONFINEMENT FUSION EFFORTS

G. W. Kuswa

ERDA, Washington D.C.

The goal of the ERDA inertial confinement program is to produce thermonuclear burn in small pellets and develop applications. Main-line efforts are being directed to achieve pellet implosions with neodymium glass lasers, CO_2 lasers, and electron beams. Various schemes for employing ion beams are also under study because of the favorable energy deposition properties of ions, which exhibit maximum dE/dx near the end of their range.

One can see by examination of the graph below the spending distribution among the various funding categories. Not shown is the result of a recent decision to double support for diagnostics to accomodate new requirements and ideas brought about by the current target interaction experiments. A balanced national effort takes advantage of the following:

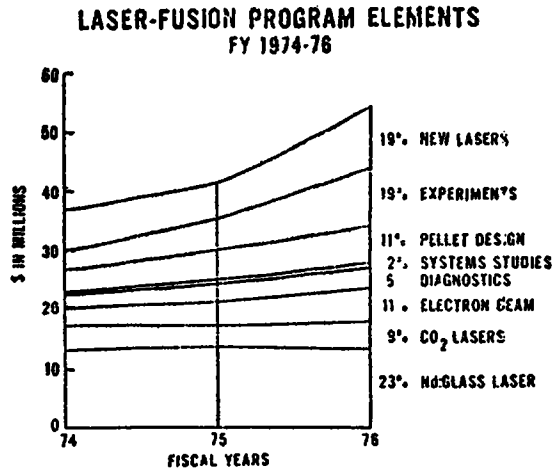

I. Utilization of Unique ERDA Laboratory Expertise (Primarily at LASL, Sandia, LLL)
   - over 20 years experience with TN burn
   - experimental diagnostics base
   - management of large applied science and research and development edeavour
   - large computers
   - sophisticated codes

II. Utilization of industrial and university expertise
   - laser and optical development
   - more ideas stimulated and incorporated
   - industrial research capability
   - fabrication technology for hardware and diagnostics

III. Development of Capability that Extends Program
   - development of pool of trained experts
   - preparation by partnership for industrial takeover when commercial implementation becomes feasible.

The inertial confinement program office at ERDA is planning on funding about 70 external contracts during the fiscal year 1976 in order to implement the philosophy outlined.

The major program goals and milestones are outlined in the figure below but one should bear in mind that the program is under continuing review and the

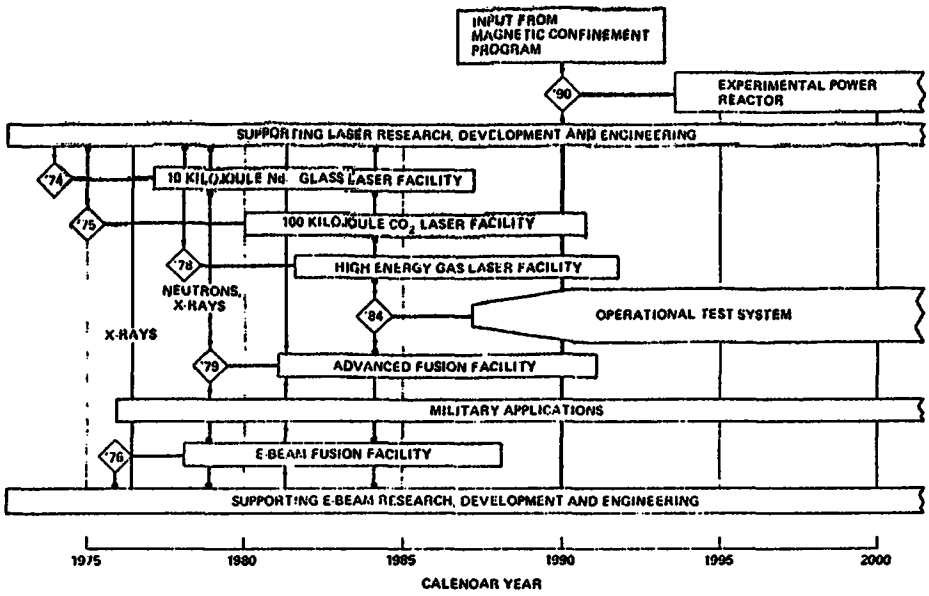

more distant projects and dates are subject to change. New laser development is required for eventual commercial power production because it is expected that pellet gains of ~100 will be optimal for reactor design. (Preliminary system studies show advantages for producing high frequency of small pellet explosions rather than a lower rate of larger explosion). Gain including the laser efficiency and pellet gain is shown on the graph below plotted against a multiplication factor for fission blankets of various kinds. The slauted straigt lines show recirculating powers of 10, 25, and 100 % based upon all internal energy need to run the inertial confinement plant. The curve is shown through points which correspond to estimated requirements for stages of fusion plant design, and present or projected laser development are also shown. Electron beam efficiencies are presently such that the range labeled "new lasers" may equally well refer to electron beam technology.

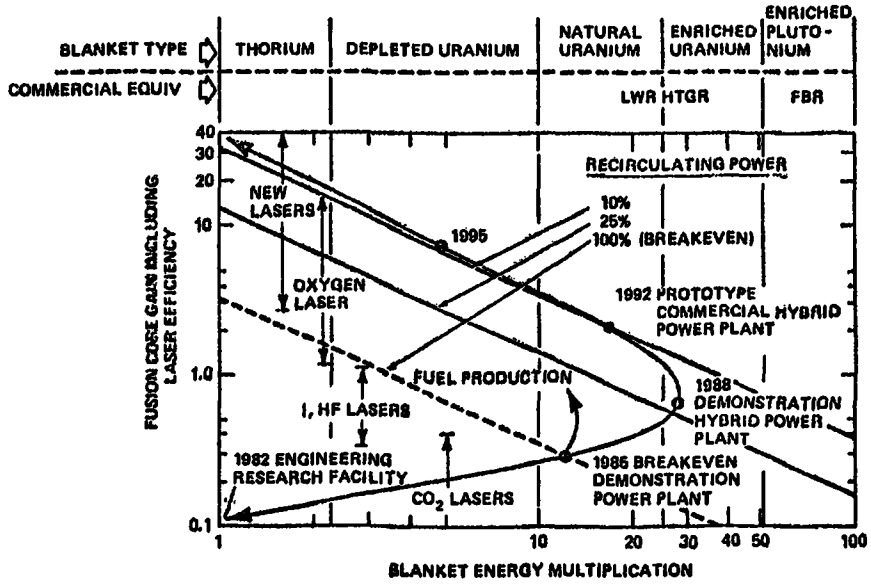

Glass systems

Despite difficulties with glass laser systems they are in the most refined state of engineering and are currently the work-horses of laser fusion experiments. The most important measure of a laser is power on target. Power is limited by the tendency for glass to exhibit non-linear properties at high intensity levels. This results in the break up of the beam into filaments of high intensity and divergence, which can cause a beam to have its own target power minimized at peak laser power. Careful attention to laser design such as the use of spatial filtering, improved glass with high gain and lower non-linear index, and design of focusing optics to minimize glass length are required. Pulse shaping is important for many pellet designs. Means for producing nearly any desired pulse shape from a given oscillator pulse have been developed but mode locked oscillators to produce the original pulse are presently not as reliable as desired. Effective isolation of lasers from damaging back-scattered light and isolation of the target from fluorescence of the laser or unwanted precoursor pulses from the oscillator is very important. Presently, experiments which produce neutrons are critically dependent upon minimizing prepulses.

Gas lasers

Gas lasers are superior in principle to solid state lasers because damage to the medium is not possible and parameters can readily be changed. Presently the CO_2 is the farthest developed and a one nonosecond 100 kilojoules facility is planned. Development of multilines oscillators, needed for efficient energy extraction in pulses shorter than the relaxation time between adjacent laser levels, has shown that this can be accomplished, but reliability is still not as good as required. Isolators for keeping prepulses from targets must also be perfected for CO_2 lasers, which have a broad spectral output due to multiline operation.

Electron Beams

Electron beam technology can currently deliver energy stored in capacitors to electron beams with efficiencies of 50 %, and this energy can be focused onto targets and absorbed with up to 50 % efficiency. However, e-beam targets require walls sufficiently heavy to stop electrons.
Appartently the only neutron producing shots employ fast rising pulses, for which plasma clouds surrounding the pellets are small. This permits electron clouds to exist during the laser burst, and such clouds may accelerate ions to energies sufficient to explain a large share of neutron production. Longer prepulses produce more extensive plasma or neutral particle distributions which cannot support the electric fields necessary for accelerating particles to neutron producing energies. More work remains to settle this important question. A large quantity of energy is required to drive e-beam pellets. Currently electron beam technology permits the study of energy deposition symmetry and material properties under shock conditions, and studies in these areas are being actively pursued, primarily at Sandia Laboratories.

The development of larger e-beam accelerators with shorter pulses of higher current is continuing. The major difficulty associated with scale up is delivery of the electrical power across the insulator which separates the vacuum region of the e-beam diode from the transmission line. To accomodate large power flow the diode insulators must be made larger and the diode electrodes must also be made larger to minimize the inductance of the system. In such large diodes it may be more difficult to control the accuracy and rise time of e-beam focussing. It has been found experimentally and theoretically that plasmas and ions formed on the diode surfaces profoundly influence the e-beam dynamics. It may be possible to control the beam by

artificial introduction of plasmas into the diode and some encouraging progress has been made in this direction.

Diagnostics.

The e-beam program relies heavily on pin hole X-ray photographs to examine the uniformity of e-beam deposition on pellets. The most notable recent progress has been in the application of computer image enhancement techniques for maximizing the information from the data. To accomplish this point spread functins of the pin holes are obtained using an X-ray source of similar energy to the experiment, and the computer program uses this data in the unfolding process. The same technique may be useful in the laser pin hole experiments.

A means for obtaining flash X-ray pictures of imploding e-beam pellets using an auxiliary pulsed X-ray source has been employed and is being used to compare experiments with theoretical models of pellet dynamics.

Other important diagnostics include doppler interferometry to study rear surface breakup of half-pellets or slabs, multipulse optical holography to examine plasma motion in diodes, and spectroscopic techniques to aid in further determining plasma properties.

The laser program relies on a somewhat different diagnostic base. Study of reflected and scattered light from pellets at the input wavelength and its harmonics allows one to learn about the light absorption properties in the outer regions of the pellets. Streak cameras are used to record the time dependence of this light. Improvement of streak camera performance and reliability is an important activity in the program.

Currently the devleopment of grazing incidence X-ray optics is being carried out to improve the collection efficiency in X-ray imaging by a factor of 10^3 over a pin hole of equivalent resolving power. Resolution in the one micron range is anticipated with sufficient sensitivity to allow streak camera recording of X-rays produced during the pellet implosion. A new streak camera development will probably result in $\sim$ 5 picosecond resolution of X-ray production.

A variety of charged particle collectors and energy analyzers are employed and recent emphasis is on improving the ability of these instruments to yield quantitative data on particle numbers. This requirement is more difficult than it appears at first because of the pulsed nature of the experiments and problems with secondary emission in the collectors and detector sensitivity which varies with charge state, mass, or energy.

Neutron detection is important, but present neutron yields are insufficient to get accurate information on the DT temperature. Consequently heavy reliance is now being placed on alpha energy measurements from the DT reaction. One factor which may not be completely known presently is the effect of the pellet wall at elevated temperatures on the alpha energies. Stopping power measurement of thin films heated by laser pulses may be desirable.

The large quantity of data generated, not only by the pellet, but also by the laser or e-beam accelerator on each shot places an unmanageable burden on the investigators. Consequently there has been a steady increase on the use of on-line computers for data reduction. The refinement of interfaces between diagnostics and the computer is being pursued on the larger experiments.

Pellets.

The design of pellets is too complicated to summarize and is carried out primarily in the main ERDA laboratories. The theoretical developments are placing increasingly more difficult burdens on fabricators. For instance one result asks for pellet finishes as smooth as the interatomic distance of the material. It is not known whether this requirement is realistic in view of the difficulty in uniformly illuminating pellets and the only partially known effect of smoothing the implosion by electron thermal conductivity in the presence of self generated magnetic fields.

Pellet selection and fabrication relies on a collection of innovative techniques, but we have been somewhat limited by relying primarily on available glass microspheres used for filling plastic commercially. Work is under way to fabricate shells made of other materials. The technology of producing small liquid DT spheres and aim them accurately is partly in existance, and work is continuing in several laboratories to freeze uniform distributions of DT on the inside surface of glass microspheres.

Conclusion.

While there has been exceedingly rapid progress in inertial confinement, and several laboratories are producing neutrons, we must still remain cautious in our interpretations of the data.

Several mechanisms have been suggested for producing populations of fast ions which may be responsible for producing neutrons. It should also be emphasized that present experiments are thought to operate in a regime which starts on a rather high temperature adiabat so that the high compressions required for high gain fusion are not obtained; hot plasma far from conditions required for thermonuclear ignition produces the neutrons.

If the present neutron yields are of true thermonuclear origin, we may still have to overcome problems of instability and mix of shell material before high gains become possible. In anticipation of these possible problems it would be desirable to put more emphasis on obtaining high quality data on stability, material breakup and mixing, and the associated theory.

LASER FUSION RESEARCH AT THE CENTRE D'ETUDES DE LIMEIL, FRANCE

J.P. Babuel-Peyrissac and J.P. Watteau

The main results obtained at the Centre d'Etudes de Limeil on laser interaction, implosion and numerical simulation are presented.

Laser interaction at 1.06 μm on solid D_2 plane target was studied over the range 10^{12} - 5.10^{14} W cm $^{-2}$. For laser flux less than 10^{14}W.cm^{-2} absorption seems to be classical; from resonant absorption near the critical density, $2\omega_o$ light is emitted and permits the evaluation of the focus spot size. Above 10^{14} W.cm^{-2} absorption becomes anomalous and hard X-rays are observed with energies up to 270 keV; this anomalous behaviour may be due to the onset of the Brillouin backscattering instability. To study the interaction at higher fluxes, a 100 ps laser called P 101 was built, the last amplifier containing 80 mm disks. 10 J at the end of the laser and 6 J at the target are obtained, but the disks are rapidly damaged by burning particles coming from the clading which absorb a great part of the flash lamp UV light.

At 10.6 μm and with fluxes of a few 10^{12} W.cm^{-2} on solid D_2 , reflection is of the order of 60%, 10% being reflected inside the focusing lens solid angle, and fast ions detected.

In QUATOR implosion experiments, CH_2 or Al hollow cylinders were illuminated by the four beams of the 500 J - 3ns Nd glass laser C_6. The diameter and thickness of the cylinders vary respectively from 200 μm to 1 mm and from 25 μm to 100 μm, and laser flux is up to 10^{14} W.cm^{-2} . From visible light pictures, interferrograms at 0.53 μm and ions collectors, the ablated corona plasma expands symmetrically when the beams are defocused and overlaps the transit time of the induced shock through the tube wall thickness and its time to converge on the axis, are deduced from the dynamical behaviour of the plasma expanding inside the tube from the inner wall towards the axis. The visible light emitted by this plasma or the attenuation of a coxial 0.53 μm laser beam are rewided along a diameter by a streak camera. From the transit time and knowing the equation of state for the cylinder material, pressure was evaluated to be of the order of 2 Mbar. The average velocity of the expanding plasma is 5.10^6 cm s^{-1} which, according to numerical simulation should correspond for Al with a density compression ratio of 10 on the axis.

We are now preparing spherical implosion experiments by putting a 90 mm diameter rod amplifier in front of the last 64 mm diameter rod in each beam. The energy of the C_6 laser is increased by a factor of 2 with the pulse duration remaining the same. The four beams are synchronized on target with an accuracy of 50 ps, each beam delivering about 150 J in a repeated way at that time. The first integrated X-rays pinhole pictures of the 150 μm diameter CH_2 spheres held by 10 μm diameter supports show that these supports absorb part of the laser energy and perturb the implosion which is no longer symmetrical. The supports must be changed to a few μm diameter.

The implosion is studied analytically and numerically. For isotropic and homogeneous compression pressure and laser power laws are found as similarity laws which help improving the efficiency of numerical simulation or preparing experiments.

Using a two fluids one dimensional code, implosions of spheres or shells in DT or in CH_2 were simulated for different laser pulse shapes

(step, ramps, gaussian, Nuckoll's law) and an energy of a few 100 J. For spheres it is necessary to deliver an important part of the laser energy in a short time at the end of the implosion to obtain high pr product. For long pulses the efficiency is best for shells when mass is fixed, but the final density and temperature depend greatly on the pulse shape, e.g. the Nuckoll's law exponent. For Al shells filled with DT on D_2 gas an optimal thickness is found for which the absorbed energy is well transferred from the shell to the gas without excessively increasing its enthropy.

Finally in order to optimize the coupling of the C_6 laser and targets, numerical simulations are done with the hypothesis that only half of the laser energy is absorbed. For 150 /um diameter CH_2 sphere, 150 J absorbed and 180 GW maximum power the average density compression ratio ρ/ρ_0 (with respect to the solid density ρ_0) is 8 and the average temperature T is 19 eV. When the maximum power is increased to 330 GW, the gaussian pulse duration being 500 ps, ρ/ρ_0 and T are respectively 18 and 74 eV for a 80 /um diameter sphere absorbing 94 J. In this last case, with a 10 GW-3ns prepulse ρ/ρ_0 goes up to 30; for a $\frac{\Delta r}{r} = 5$ aspect ratio shell having the same mass, ρ/ρ_0 and T are 44 and 140 eV, and maximum values of 69 and 710 eV are attained in the center of the hard core.

LASER FUSION RESEARCH IN THE UNITED KINGDOM

I. J. Spalding

UKAEA Culham Laboratory

There is no laser-compression experiment at the UKAEA Culham Laboratory. There is, however, a very active interest in the laser-heating of plasma for filling toroidal magnetic-confinement devices, and in the diagnostics of dense plasmas. A wide range of related laser work, for lower density diagnostics and other applications, is also undertaken within the Laboratory; longer-term exploratory work is supported by Culham at nine UK universities. The present performances of some typical Culham facilities are listed below. (Projected performance is indicated in parantheses)

LASER	WAVELENGTH (μm)	ENERGY (J)	POWER GW	MODE STRUCTURE	APPLICATION
1. $C^{12}H_3F$	496	-	3×10^{-3}	Multi	Tokamak diagnostics
"	"	(0.3)	(3×10^{-3})	(single)	" "
2. CO_2	10.6	1	1	single	Heating/Diagnostics
"	"	150	2	multi	Heating
"	"	(1000)	(1-200)	(single)	Heating
"	"	large	10^{-6}	(continuous)	Industrial
3. Nd/glass	1.06	$\leq$ 50	(100)	single	High density diagnostics
4. Nd:$POCl_3$	1.052	50-60	3	multi	Heating

It may seem strange to mention a (continuous) 10 kW laser in a laser-fusion context, but design experience with higher mean power systems of this type helps one to appreciate the technological challenge of laser-fusion; I will reserve comment on some implications of using multi-shell cryogenic targets in a reactor environment until the reactor session on Friday.

The laser-heating programme (Spalding and co-workers) forms part of a co-operative Euratom venture[1]; Culham is initially using a 160 litre-atmosphere electron-beam preionized CO_2 laser for this work, which will be discussed in detail on Wednesday. Recent work includes laser-induced acceleration of pellets to velocities of 10^4-10^5 cm/sec (for refuelling investigations), computer-modelling of CO_2 laser pulse-propagation[2], and an experimental investigation of density-cavity ('caviton) formation at incident CO_2 laser intensities of order 10^{13} W/cm^2.[3] A very important objective of the programme is the optimization of the energy transfer between laser and target - a problem which is closely related to non-

linear coronal interaction physics of current interest in laser-compression experiments, described by other workers at this meeting.

The high-density spectroscopic investigations at Culham are being conducted by Peacock and colleagues. A primary objective of this work is to obtain a quantitative fit between x-ray measurements[4] and two-dimensional MHD computations of the general type discussed in Reference 5.

I. J. Spalding

References

1. 'The present state of research into Plasma Heating and Injection Methods'. Euratom Report EUR FU 74/AGHI 10/R1 Section 5(c).
2. 'Pulse propagation in CO_2 laser amplifiers'
   Armandillo E and Spalding I J, to be published in J Phys D, Appl Phys (Culham Report CLM-P423)
3. 'CO_2 laser-heating experiments'
   Donaldson T P et al.
   Proceedings of 7th European Conference on Controlled Fusion & Plasma Physics, Lausanne, Switzerland (September 1-5 1975).
4. 'Spectral classifications in the Fe XIX to Fe XXIII isoelectronic sequences'
   Fawcett B C, Galanti M, Peacock N J, J Phys B Atom Mol Phys 7, 1149 (1974)
5. 'X-ray emission from laser-produced plasmas', C
   Christiansen J P, Peacock N J, and Galanti M, Lausanne Conference (Sept 1-5 1975).

Laser Research at the Institute of Applied Physics University of Berne (Switzerland)

H. Weber

The Institute of Applied Physics includes three main activities:
Microwaves (Prof. E. Schanda), fluorescence (Dr. T. Binkert), and the laser group (Prof. H. Weber). In the following a brief review on the activities and facilities of the laser group will be given. The program and present status of the laser-plasma group will be presented in more detail.

Facilities, Activities, and Program of the Laser Group

In the summer 1963 the work in the laser field started with a few collaborators who organized the International Symposium on Laser Physics and Applications in Berne in 1964. Today the laser group consists of about 30 scientific members including Ph.D. students and technicians. Investigations in the laser field are carried out in close contact with several industrial companies. Therefore the activities of the laser group may be divided into basic research and applied research. This partition is not a very strong one, because these two fields are closely connected and stimulate each other.
The laser group has become one of the laser centers in Switzerland. Thus, our laboratory is constantly confronted with many problems concerning laser applications. As it is impossible to treat all these problems within an university laboratory, the Applied Physics Institute in collaboration with some Swiss industrial Companies have founded the LASAG Inc., an organization which studies practical laser applications on a commercial basis in consultation with the Institute of Applied Physics.

Coherent Optics (Dr. T. Tschudi)

Application of holography and interferometric techniques on quality control, development of holographic methods for plasma diagnostics.

Diode Lasers (Dr. R. Salathé)

GaAs-diodes for range meters, mode-locking, single frequency diodes, technology of diode preparation.

High Power Gas Lasers (Dr. W. Seelig)

cw-Argon (100 W) and Mercury systems, CO_2 laser with mode-controlled output for material processing and plasma generation.

Interaction (Dr. T. Tschudi)

Nd-YAG and CO_2 laser interaction with metal. Investigation of optimum parameters for material processing with moderate laser systems (10^7 - 10^9 W/cm^2, $\tau = 10^{-6}$ - 10^{-8}s).

Short Pulses (Dr. M. Keller)

Mode-locked dye lasers for plasma diagnostics, modulation of lasers (periodic Q-switch). Satellite ranging and illumination.

Laser Plasma Group (Dr. W. Seka)

Interaction of picosecond pulses with matter, investigation of reflectivity, absorption, and plasma instabilities. The laser system for the interaction is under construction and will be finished this year. We hope to start with the plasma investigations at the end of this year.

Laser System (fig. 1)

Mode-locked ring oscillator with Nd-YAG rod. Stable resonator configuration (resonator is insensitive to disturbance by thermal effects of the rod). Emission of a very reproducible mode-locked pulse train, Gaussian shape in time, frequency, and spectrum. The pulse is bandwidth limited, $\tau = 35$ psec. The spatial structure is monitored by an array.
Single pulse selection by KD* P electro-optical switch, improving the signal to noise ratio by a discrimination amplifier. Power and energy amplification by Nd-YAG

preamplifier and two ND-Glass amplifiers, one of those is under construction.
The output energy is about 0.1 Joule at the moment, at the end of this we hope to achieve 1 Joule.

Diagnostic Tools and Vacuum Chamber

At our disposal are

- fast streak camera (Hadland)
- fast X-ray diode
- X-ray - Bragg spectrometer
- ion collector
- vacuum chamber (10^{-8} Torr)

A grating spectrometer for the 100 Å region is under construction.

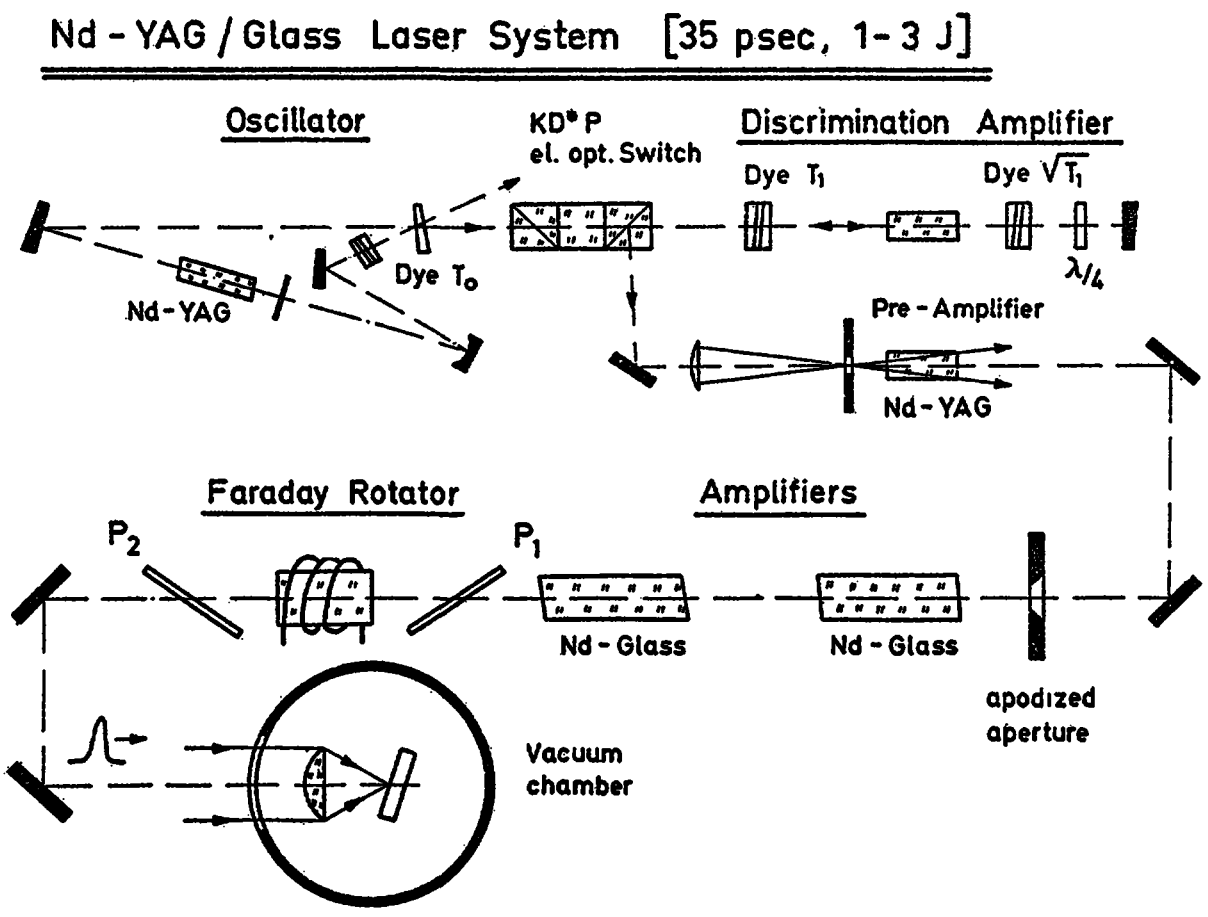

Fig. 1 Nd-YAG - Glass laser system for generation and investigation of plasmas.

NATIONAL AND LABORATORY REPORTS

Electron-beam produced fusion

RESEARCH AT THE I.V. KURCHATOV INSTITUTE OF ATOMIC ENERGY ON THE USE OF POWERFUL ELECTRON BEAMS TO INITIATE A PULSED THERMONUCLEAR REACTION

L.I. Rudakov

In view of the relatively high penetrating capacity of electrons, thick sheaths (0.1–0.3 mm of lead or copper for 1–3 MeV electrons) are required for stopping them. Ignition of a thermonuclear reaction requires acceleration of the sheath containing and heating the D–T mixture to a velocity of over 150 km/s. In order to utilize all the energy of the beam, of duration 50 ns, for the acceleration of the sheath, the initial radius of the target must therefore be about 1 cm. These conditions allow evaluation of the mass of the target sheath, (1–3 g), and of the energy required for its acceleration (10–20 MJ). When the D–T mixture is burnt in such a target, a thermonuclear energy of 10^9–10^{10} J can be obtained. With the target dimensions quoted, the duration of beam action on the target corresponds to the range of pulse durations of existing accelerators. It is quite feasible to obtain an energy of the order of 2×10^7 J in the beam at the present stage of technical development.

The pulsed thermonuclear reactor design developed by E.P. Velikhov, V.V. Chernukha et al. at the I.V. Kurchatov Institute of Atomic Energy [1] foresees introducing into a capsule construction injected into the reactor a massive screening sheath for neutron absorption and retardation, which would serve as the working body in the energy conversion cycle after evaporation. This permits a significant reduction of damage to and activation of the walls of the explosion chamber by neutrons, and prolongs the service life of the chamber to 20–30 years, which corresponds to the usual standards in electric power plants.

At a sufficiently high explosion energy ($\gtrsim 10^{10}$ J) the material of such a sheath can be heated to 10^4°K, which permits use of highly effective thermodynamic cycles, e.g. the MHD method of conversion, by which a power plant efficiency of 70–80% can be obtained.

An explosion energy of about 10^{10} J can be contained in chambers with a diameter of 20–30 m, and a weight of 500–1000 t; such chambers can be constructed in the present state of technological development. Assuming that the energy conversion coefficient will be of the order of 10^2–10^3, initiation of such a thermonuclear explosion requires an energy of $\gtrsim 10^7$ J in the electron beam.

An accelerator of electrons with an energy of $(2\text{–}3) \times 10^7$ J in the pulse and a power of $(2\text{–}3) \times 10^{14}$ W might for instance consist of a number of modules arranged around the vacuum chamber, as shown in Fig. 1.

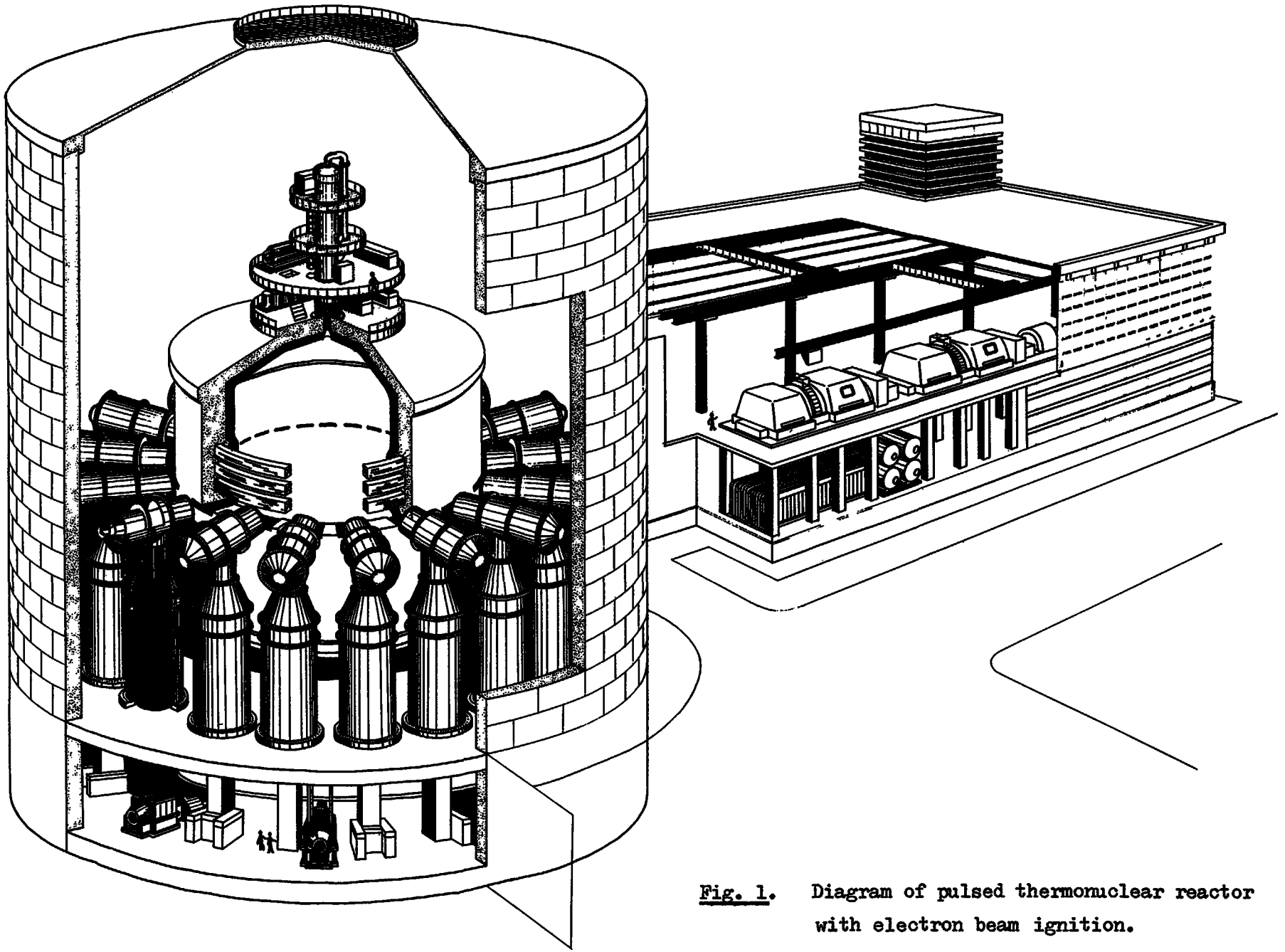

Fig. 1. Diagram of pulsed thermonuclear reactor with electron beam ignition.

If an accelerator with a power of 3×10^{12} W is selected as the individual module, 60–100 modules will be required. The parameters of such a module would be close to those of existing accelerators.

With an output voltage of ~ 3 MV the total current in the device should be of the order of 70–100 MA. It is known that a diode current cannot exceed a certain critical value.

$$J \approx 10^4 \frac{r}{d} \gamma,$$

where r is the cathode radius, d the anode–cathode separation, and γ the relativistic factor.

When d = 1 cm and the module outlets are closely packed, a current of 70 MA can be achieved over a radius of 5–10 m. This corresponds to the requirements for the explosion chamber.

The construction of accelerators giving 10^7–10^8 J under pulsed conditions and their use to trigger a pulsed thermonuclear reaction require the solution of a number of physical and technical problems. The technical problems include synchronization of multichannel switching, beam inlet into the explosion chamber, development of outlet window shielding, foil exchange or evolution of an anodeless procedure for introducing the beam through the opening with a suitable system of differential evacuation to maintain the vacuum in the diode.

The fundamental physical problems are transporting the beam to the centre of the vacuum chamber over a distance of the order of 5–10 m, and the effective irradiation of the thermonuclear target. The problem of transporting the beam may be solved by using a guiding magnetic field and admitting gas into the chamber to produce a plasma tube for electrical and magnetic neutralization of the beam [2]. As a guiding field, a cusp configuration – a field from two coils connected in opposition – can be used. In the explosion and target expansion stage this magnetic field can be used for MHD-conversion of the explosion energy into electrical energy.

The modular design of the accelerator makes it possible to handle all the technical and a number of physical problems full scale on an individual module; in particular, it is possible to simulate irradiation of the target from all sides in the vacuum chamber within the high-voltage annular diode (a diagram of such an experiment is given in Fig. 2).

The problem of producing a powerful beam, of transporting it and of irradiating the target was studied at the Kurchatov Institute on the specially

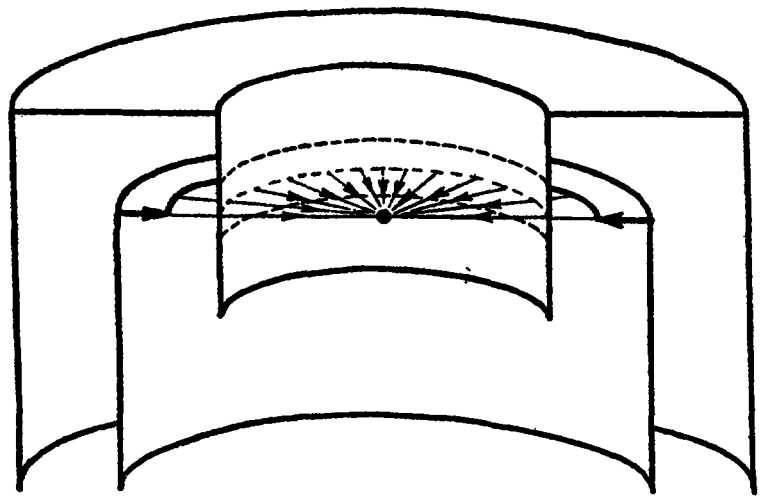

Fig. 2. Diagram of diode simulating target irradiation from all sides.

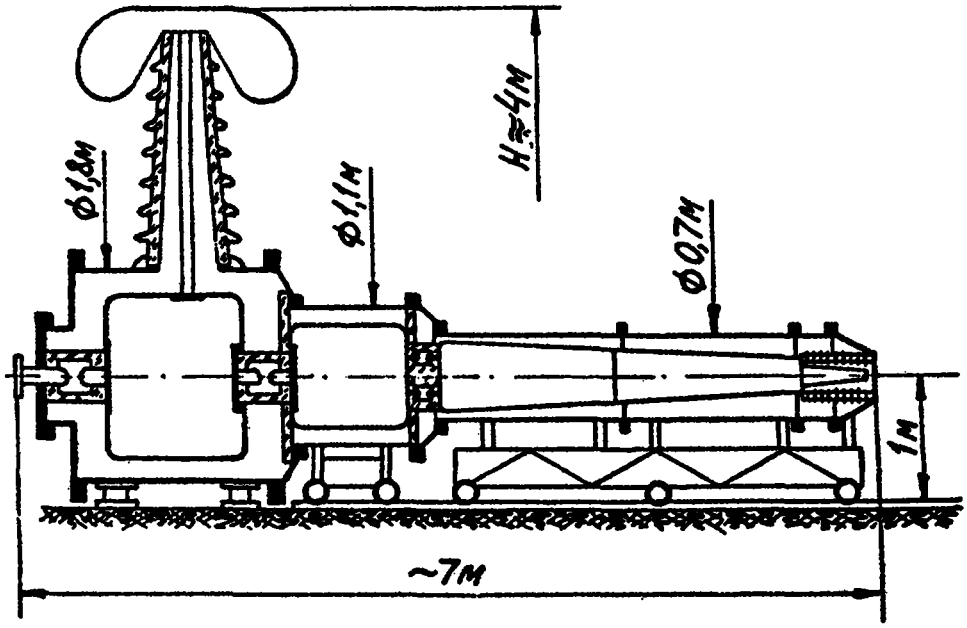

Fig. 3. Diagram of Angara-1 device.

designed Angara-1 device (Fig. 3), which is calculated for obtaining an electron beam with an energy of up to 2.5 MeV and a current of up to 400 kA for a period of 60 ns. It consists of a three-stage single water line charged by a separate air-type voltage pulse generator with an energy capacity of up to 150 kJ and a voltage of up to 2 MV. The Angara-1 device began operating in February 1975.

Production of the necessary power density in the beam on entry into the explosion chamber requires increased electrical stability of the line.

Experimental research on the efficiency of magnetic insulation was carried out on the "MS" accelerator. A voltage pulse with an amplitude of up to 400 kV was transferred to the accelerating gap cathode across a section of coaxial vacuum line. It was shown that with sufficiently high currents in the line an electric field density exceeding the breakdown value is reached in the line when the magnetic field itself exceeds a certain level. In gaps of 2 mm an electrical density of up to 2.5 MV/cm and a power flow density of ~ 10^{10} W/cm^2 was recorded [3].

On a number of small-scale devices with low wave resistance of the forming lines ($\varrho \lesssim 2.5$ ohm), self-focusing regimes of high-power beams in diodes were investigated. On the "Triton" device, the current density of the beam reached 5 MA/cm^2 with a total current of 200 kA. On the "Ural" accelerator a current density of up to 30 MA/cm^2 was reached with a beam current of 90 kA and an energy flow density of 5 x 10^{12} W/cm^2 [4]. At present, acceleration of thin films under the action of electron beams is being studied on the "Triton" device. The efficiency of beam energy transfer to a spherical target as shown in Fig. 2 is being investigated on the "Ural" device.

In 1976-77 these experiments will be repeated on the Angara device at a level of 30-56 kJ, and in 1978-80 at 100-200 kJ. These experiments should yield information on the efficiency of the chosen system of initiating the pulsed thermonuclear reaction and on the appropriateness of building a multimodule device for an energy of 3-5 MJ in the electron beam.

REFERENCES

[1] VELIKHOV, E.P., GOLUBEV, V.S., CHERNUKHA, V.V., At. Ehnerg. 36 4 (1974) 258.

[2] BABYKIN, M.V., ZAVOJSKIJ, E.K., IVANOV, A.A., RUDAKOV, L.I., Plasma Physics and Controlled Nuclear Fusion Research, IAEA, Vienna, V. I, (1971) 635.

[3] GORDEEV, A.V., KOROLEV, V.D., SIDOROV, Yu.L., SMIRNOV, V.P., paper presented at Conference on electrostatic and electromagnetic plasma containment and on relativistic electron beams, New York, March 1974.

[4] KOBA, Yu.V. et al., in: IAEA-CN-33/F 2-1, Fifth International Conference on Plasma Physics and Controlled Nuclear Fusion Research, Tokyo, Japan, 10-15 November 1974.

ELECTRON BEAM RESEARCH AT SANDIA LABORATORIES, USA

G. Yonas

I. General Description of Program

Sandia Laboratories is engaged in an effort involving thirty scientists to investigate the feasibility of using intense electron beams to achieve inertial confinement fusion. The long-range goal of this effort is to demonstrate scientific breakeven during the early 1980's. To this end, an experimental and theoretical program is being followed including the development of electron accelerators of increasingly higher power. This approach is being considered as an alternate method to the use of lasers for ignition of fusion reactions in imploded pellets for power production, because of the relatively high efficiencies which can be achieved with electron accelerators (up to 50%).

The major technical questions which are being considered are as follows: delivery of intense beams to targets of a few mm diameter; efficient energy absorption; symmetry of ablation; and stability of spherically imploding shells.

The concept of using either one or two beams within accelerating diodes is being considered, using hollow cathodes and preformed anode plasma to provide charge neutralization. In order to minimize the distance of beam transport from the hollow cathodes to the target and maintain a low diode inductance, it is necessary to maximize the breakdown strength of the dielectric interface through which energy reaches the vacuum diode, and to increase the attainable electric fields in the vacuum-insulated section feeding the emission region. The goal of these studies is to deliver $\sim 10^{14}$ W at 1 MeV from diodes of $\sim$ 1 M radius. Target design studies employing ablator-pusher concepts indicate that $\sim 10^{14}$ W in a 10-20 nsec unshaped pulse will be required to achieve

breakeven; and systems analyses show that, at this level, net power production could be achieved with an accelerator efficiency of 50% and a hybrid blanket gain of $\sim$ 20. A pure fusion reactor would require a pellet gain of at least 10 implying the need for (1) more complex target designs to lower the input power levels, or (2) if nature is benevolent, a non-classical electron deposition profile so that higher voltage electron beams can be used, or (3) the use of intense ion beams.

II. Theoretical Program

A. Diode Physics: Multi-dimensional particle-in-cell simulation codes have been constructed in cylindrical, conical, and spherical geometries including electrode plasma, self-consistent electron and ion flows, self-consistent fields, and emission laws. These studies have shown the importance of ion production in predicting beam pinching and in determining impedances and focusing; they also indicate that in certain cases the self-pinched electron beam can lead to ion currents equal to or even greater than the electron current. Such ion beams might be geometrically focused for use in ion beam fusion.

B. Fluid Models: Solutions of fluid equations giving radial equilibria have been obtained to study focusing limitations and conditions of symmetry on targets. This work indicates that a 25% variation in energy flux should be expected on a hemispherical target slightly smaller than the beam, and a two-to-one variation on a target slightly larger than the beam.

C. Hydrodynamic Code Modeling of Target Response: A 2-D Eulerian hydrodynamic code including mixed phase equations of state, elastic-plastic effects, and fracture has been used to relate target response to beam parameters. Electron deposition is treated using a 2-D Monte-Carlo

treatment including effects of magnetic fields. Predictions of crater formation and shock wave intensities in slab targets and implosion characteristics of hemispherical and spherical targets indicate correlation with efficient classical absorption and symmetry levels as good as $\pm$ 10%.

D. Target Design: Design studies are performed with a three-temperature, 1-D Lagrangian code including radiation and thermal conduction. Calculations have included high-z shells (pushers) used to compress DT gas with low-z ablators, as well as multiple shells for velocity multiplication. These studies indicate that breakeven should be possible at $\sim 10^{14}$ W with $\sim$ 1 MeV electrons or $\sim$ 10 MeV protons. The ion beam approach would allow roughly an order of magnitude reduction in the beam current and would permit the target to be injected into a vacuum chamber as in laser fusion with no additional plasma required. Charge neutralization would be provided by cathode plasma electrons dragged by the non-relativistic ions into the vacuum region.

III. Experimental Program

A. Hydra: The Hydra accelerator uses a conventional Marx generator to charge two 80 nsec long, coaxial, water insulated transmission lines providing up to 0.8 MV, 0.4 MA, from each line. This accelerator can be used in a single beam mode or the two lines can be triggered with $\sim$ 5 nsec jitter to deliver two beams to a single target using curved, magnetically insulated, coaxial vacuum transmission lines. Recent experiments have emphasized shock response of slab targets, with holographic and other optical measurements of front and rear surface motion indicating classical deposition. Implosion time and jet velocity of hemispherical targets absorbing 5-10 kJ have indicated 2:1 asymmetries in beam deposition. More diffuse beams have been used to implode spherical targets

with 2-3 kJ absorbed and interferograms of ablated material indicated symmetry as good as $\pm$ 10%. Experiments with CD_2 targets indicate neutron yields of 10^7 - 10^8, thought to be a result of collectively accelerated ions. Future spherical implosion experiments are planned using pulsed flash x-ray shadowgrams, to correlate the implosion quality with time resolved neutron yields.

B. Proto-I: (Operational 1975) -- The Proto-I accelerator which has recently been operated for the first time, is projected to deliver two 3.0 MeV, 400 kA, 24 nsec beams with two opposing cathodes to a target in a common anode. This device uses twelve oil insulated pulse forming lines which are triggered with a switch jitter of less than 2 nsec. The output current risetime of 10 nsec will permit studies of rapid beam pinching from cathodes of diameter up to 60 cm, using a preformed anode plasma. Proto-I may also permit the generation of several hundred kA ion beams which could be conveniently extracted through the cathodes (at ground potential) for diagnosis.

C. Proto-II: (Operational 1976) and EBFA (proposed -- operational 1979)

Proto-II, which is in an initial development phase, has design characteristics of 1.5 MeV, 3 MA, 24 nsec from each of two beams. This device employs sixteen pairs of untriggered water insulated pulse forming lines in order to provide a power output of 8×10^{12} W with a risetime of $\sim$ 10 nsec. Proto-II will test design concepts for use in a 4×10^{13} W accelerator (EBFA) which has been proposed for completion in 1979 and should also permit the production of 10^8 - 10^9 neutrons per pulse in order to carry out detailed studies of DT fuel compression and heating by imploding shells. EBFA should be able to achieve significant thermonuclear yields. With a further upgrade to 10^{14} W or greater (projected for the early 1980's) scientific breakeven can be reached if the technical obstacles mentioned are successfully overcome.

IV. Summary -- Electron Beam Fusion Research

In summary, the Sandia emphasis for inertial confinement fusion is on use of a minimum number of accelerator modules and avoidance of beam transport in external fields. This approach is a consequence of numerical modeling as well as recent experimental demonstrations of beam self-focusing, efficient energy deposition, and beam symmetry on targets. They propose to use $\sim$ 10 nsec, 10^6 J pulses to achieve breakeven with a fuel mass of 10^{-4} g. Present experiments involve focusing of beams from two hollow cathodes onto a single pellet with studies of implosion symmetry and stability using optical and x-ray techniques. Recently they have also suggested that self-focused electron beams may provide comparable ion currents, permitting an order of magnitude reduction in required currents as a result of improved deposition characteristics.

The Soviet effort of the Kurchatov group is directed toward beam transport in a plasma with an externally applied magnetic field. In this way they hope to make it possible to use a multiple module approach with relatively minor advances in high voltage accelerator technology. In addition, by transporting as many as twenty, 0.5 MJ beams over a distance of several meters, they envision survivable first walls with fusion energy yields of $\sim 10^9$ J. Such values of pellet gain (100) are stated to be consistent with a pellet mass of $\sim$ 1.0 gram and beam pulse duration of 50 - 100 nsec. Critical near-term experiments will involve ablation-driven acceleration of thin foil targets and studies of beam transport in cusp field geometries.

Both groups are considering only collisional energy loss in deposition thus far as there has been neither experimental nor theoretical evidence to the contrary; both groups also expect to operate 10^{14} W facilities in the early 1980's to demonstrate the true feasibility of this approach.

REB FUSION AT THE INSTITUTE OF PLASMA PHYSICS, Nagoya, Japan

A. Mohri

Experiments on the injection of REB into toroidal systems started in 1973, while ERA has been studied since 1970. For these experiments several electron beam sources are now in operation: Phoebus-I (500 kV, 24 ns, 4.652), Marx generator (2 MV, 1 kJ) and three small Marx generators (600 kV, 240 J). The source Phoebus-I has an air-core step-up transformer with a high coupling factor and it is used for the beam injection into a toroidal device named SPAC-II. Marx generator (2MV, 1kJ) serves for experiments on ERA.

Expeimental studies of the injection are summarized as follows:

1) A quescent equilibrium state of non-neutral beam ring could be realized when a relativistic electron beam (450 keV, 16 kA, 25 ns) is injected parallel to a toroidal magnetic field in a vacuum. The longest life time obtained was 20 μs which corresponds to 3000 revolutions of electrons around the torus. The electrostatic potential well was 1.1×10^4V.

2) A stable state of neutral beam ring was made when the beam was injected into neutral hydrogen gas. The obtained ring current was 7 kA and it decayed with the time constant of 25 μs.

3) Injection and heating of tokamak plasma were tried. The tokamak plasma responded in a complicated manner. The heating efficiency was about 5% and part of the injected electrons continued to circuit around the torus without fast damping.

With regard to future plans, a REB source of 10 kJ is to be constructed in the fiscal year 1975. We have another plan to make a 50 kJ source within 2 years. Using these larger sources, we will examine the interaction of REB with solid targets and also the possibility to form a toroidal ring having a spherical shape. In the latter case, the current is sustained by REB and the heating of the confined plasma is attained by three dimensional adiabatic compressions. If this system is stable, we can expect to exceed the Lawson's criterium by using an apparatus of fairly small scale.

SUMMARIES OF THE SESSIONS

LASER SYSTEMS

H. J. Doucet

Ecole Polytechnique, Palaiseau, France

A considerable part of the effort in the inertial confinement program have been devoted and is still devoted to laser systems in order to increase the laser energy and the laser power by a considerable amount.

For a futurelaser fusion reactor there is presently no ideal laser presenting simultaneously short wavelength, good efficiency, short pulse, high repetition rate, ... Nevertheless, several systems are promizing for the breakeven by laser. Present strong efforts are pursuing on several laser systems : Available power on target is increasing rapidly and is expected to grow in roughly parallel ways during the next few years for glass laser, elsctron beams and CO_2 lasers, to reach 10^{13} W around 1976, increasing later to 10^{14} W around 1984. Other systems as HF, Iodine lasers, later ions beams and X lasers will probably be also seriously considered in the inertial confinement program of the next few years.

For glass laser which provides presently the higher power, important improvement are made in laser components : Reproducibility, Beam quality including a limitation of the non linear phase shift and spatial filter, controlable pulse width, high gain amplifier are in progress despite of the numberous difficulties presented by material strength which require good optical isolation in much more complicated systems. Classical solutions like KDP cells, Faraday rotator, etc... are quite adaptable to large systems and are widely used in new systems with large diameters. A comparison betwsen rods and disks turn often in favour of rods for cheaper price and at least equal beam quality.

The CO_2 laser systems are presently improving very significantly using electron beam excitation. A few hundred joules to kJ systems in ns single pulse are already constructed. Effective extraction of stored energy in short pulse have been improved : the measured saturation parameter is explained by finite relaxation rate of rorationnal levels. Self focussing in amplifier can be avoided.

New important progress are expected in CO_2 laser components which should give to CO_2 laser systems an hopeful future in laser fusion program.

Iodine laser is still interesting for short pulse by the wavelength despite of the poor efficiency. Extraction of stored energy and repetition rate have been improved significantly.

HF lasers could be also interesting outsiders with a good efficiency and will be probably more widely studied during the next few years.

New laser systems and laser improvements are clearly needed. Some new ideas have to be checked as for instance the frequency conversion of a

high intensity of microwave radiation on the front of a relativistic electron beam which could bring a tunable very intense infrared laser with wide spectrum,very short pulse and good efficiency.

About the number of laser beams it seems presently clear that from our knowledge of symmetry properties in the energy deposition and of stability in the first stage of the target compression, the number of laser beams is mainly determined by the total required energy. Laser systems presently under studies include from 2 to 20 beams. Four beams systems are widely used and present already interesting symmetry properties in energy deposition.

INTERACTION OF LASER RADIATION WITH PLASMA

P. Sigel and V. Silin

Lebedev Institute of Physics, USSR Academy of Sciences
Max Planck Institute für Plasmaphysik, Garching, FRG

Measurements of line shapes in the X-ray region can provide important parameters of laser fusion plasmas. This was demonstrated by Tondello (Univ. of Padua) who measured electron density, electron temperature and streaming velocity of a Beryllium plasma produced by a ruby laser. The technique is now being improved by constructing a new spectrograph with a gracing incidence focussing device which allows the spectrograph to be removed from the target without loosing spatial resolution.

The interaction of intense laser radiation with the dense plasma produced in a plasma focus is under investigation at the Lebedev Institute. This investigation has essentially three aims: 1) During its first compression phase the plasma focus provides a homogeneous and dense

$$T_e \simeq T_i \simeq 1 \text{ keV}$$
$$n_e \simeq 5 \times 10 \text{ cm}^{-3}$$

plasma which can be used to study the nonlinear interaction of intense laser radiation with plasma. Such an experiment allows one to simulate the processes occuring in the corona of a laser irradiated pellet under well defined conditions. 2) Theory predicts enhanced absorption of an electron beam and reduced thresholds for certain instabilities if the target is preheated by a laser beam. These predictions can be experimentally tested during the later phase of the plasma focus where intense electron beams are known to exist in it. 3) The plasma focus constitutes an intense source of neutrons, charged particles and radiation. It thus can be used to study engineering problems of laser- and electron beam- induced fusion.

A plasma focus device with a 100 kJ condenser bank and a Nd-laser with 20 beams have been built to study these problems. The laser is designed to deliver 2 KJ in a 20 ns pulse or 200 - 400 J in a 20 ps pulse. The installation is now complete and experiments will start in the near future.

Dr. Rudakov reported on a theoretical study of solitons which might be created in the corona of a laser irradiated pellet. Laser-induced Langmuir turbulence was investigated by computer using averaging equations which include the effects of high frequency pressure on the plasma density. The main nonlinear effect in this approach is the collapse of Langmuir energy which is excited by

laser. As a result of collapse energetic electrons are produced. Some estimates of number and energy of fast electrons have been given. For example the temperature of the fast electrons scales as follows :

$$T_{e'} = \frac{q}{n\, C_s}$$

$T_{e'}$ = temperature of fast electrons
q = pumping laser flux into Langmuir waves
n = electron density
C_s = sound speed in the corona

Mr. V. Silin reviewed the results obtained at the Lebedev Institute of Physics of the USSR Academy of Sciences on the interaction of laser radiation with plasma.

Experiments on the reflection of laser radiation by plasma in conditions of parametric instability development showed that the reflection coefficient for flow density values of 10^{12}-10^{14} W/cm^2 in the case of a Nd laser in the nanosecond regime is less than 10%. In the picosecond regime the reflection coefficient was found to be greater. Investigation of the direction of the reflected radiation revealed mirror-type reflection. This showed that it is productive to use the notion of a dielectric constant of a plasma with anomalously great high-frequency conductivity depending on the amplitude of pumping. Such conductivity can theoretically change during the laser pulse, and this is demonstrated by the experimentally observed oscillations in time of the reflection coefficient. Giving a unique interpretation of such a phenomenon, and in particular separating the influence of linear and non-linear effects, requires experimental study of the dependence of such oscillations on the laser pulse wavelength, the target material, the power flow density of the radiation, etc.

Another sign of the anomalous nature of laser radiation action on plasma is the observed anisotropy of X-rays, corresponding to the appearance of electrons with a comparatively high velocity in the direction of light polarization.

Measurements at the Lebedev Institute of second-harmonic energy as a function of the flow density of laser radiation show that formation of the second harmonic is associated with the process of fusion of the transverse light wave with the longitudinal plasma wave arising as a result of transformation

of the laser radiation. The experimental relationship obtained differs from the experimental results of Siegel et al.

The concept of formation of the second harmonic as a result of fusion of the waves arising in connection with parameter effects made it possible to determine from the red shift of the second harmonic the temperature and spatial distribution of the plasma near the critical point where the second-harmonic wave originates.

Finally, notions of the ponderomotive action of an electromagnetic field on plasma made it possible to estimate the number of fast ions accelerated by the field to an energy reaching tens of keV. In a picosecond laser regime (or in the case of a picosecond structure of a nanosecond pulse) a large part of the energy of the absorbed laser radiation can be transferred to fast ions.

The difference in results obtained from the Lebedev Institute and from others may be due to the structure of the laser beam (in space and time), the contrast and other characteristics.

The Garching group has investigated the case of plane, semi-infinitive targets in great detail, to study the physics of interaction as well as to develop new diagnostic methods. Results were presented on the shockwave propagation in the target, on blastwave formation in a background gas, on density and temperature distribution in the host plasma and on reflected radiation from the plasma with frequencies CO_2, $2\omega_L$ and $3/2\,\omega$ L. The experimental studies were performed with Neodymium glass laser at intensities of $\phi \approx 10^{14}$ Wm^{-2} (20 J in 5 ns).

Evaluation of X-ray pinhole photographs shows that the hot plasma reaches an electron density of $2 - 3 \cdot 10^{21}$ cm^{-3} i.e. its density is higher than the critical density for the wavelength of the Nd laser ($10^{21} cm^{-3}$). Simple estimates show that the "cold" electrons in the plasma are not able to transport the absorbed laser flux away from the critical density layer by classical heat conduction. From an absolute intensity measurement of the hard X-ray component it has been concluded by using a simple beam-target model, that the fast electrons play an important role in the heating of the overdense plasma.

The angular distribution of laser radiation backscattered from the target has been investigated by experiment and in addition by two dimensional computer (PIC) simulation. It is found that specular reflection is unstable against collimated scatter, the transition-back being possibly induced by the parametric decay instability near the critical layer. It seems remarkable that both, experiment and computer simulation show this behaviour. From a large number of shots on different target materials and from the fact that specular and collimated losses

in backscatter are also observed in other laboratories, it is concluded that it is quite general in laser plasma experiments.

An attempt has also been made to analyse the reflection measurements made in different laboratories. A common feature of Nd and CO_2 measurements made in several European and US laboratories seems to be that up to intensities corresponding to $\frac{Vo}{Ve} \approx 0.5$ backscatter seems to be highly collimated. The reflection coefficient increases in this range despite the fact that the threshold for excitation of parametric instabilities is largely exceeded. Above $\frac{Vo}{Ve} \gtrsim 0.5$ the reflection coefficient decreases. At present it is not clear, however, whether absorption increases in proportion since in most of the experiments only reflection back through the focussing optics has been measured. There are indications that scattering losses into the solid angle outside the lens may be significant.

On the other hand measurements made at the Lebedev Institute show a quite different behaviour, mainly low reflection losses (less than a few per cent even into 2 π) and decreasing with increasing intensity. Though this discrepancy in results (obtained under similar conditions) was intensively discussed, it was not possible to identify the cause for it.

LASER HEATING FOR MAGNETIC CONFINEMENT

I. J. Spalding

UKAEA Culham Laboratory

(1) T. SEKIGUCHI (Dept. of Electrical Engineering, University of Tokyo, Japan).

Professor Sekiguchi described a collaborative programme between 17 authors in three departments of the University of Tokyo and the Institute of Plasma Physics, Nagoya University. The purpose of the programme is fourfold:

(i) To develop a fully-ionized, impurity-free, laser-plasma source, having ion energies in the kev range, for a variety of magnetic confinement devices.

(ii) To study the interaction between this expanding plasma and a magnetic field.

(iii) To study the magnetic confinement of such plasmas. (Particular attention has so far been paid to spindle-cusp confinement; see Phys. Fluids 17, pp 1895, 1974)

(iv) To study the possibility of developing an intense and compact 14Mev neutron source (10^{13} - 10^{15} neutrons cm^{-2} s^{-1}), and eventually a DT reactor, by extensions of these techniques.

Pellet source (Mark I)

Free-falling cylindrical deuterium ice pellets, having diameters of 100-400 μm and lengths of 200-600 μm (i.e. 6×10^{16} - 3×10^{18} atoms), are intercepted by a (stationary) focussed laser beam after falling freely for some 7 - 10 cm in vacuum. At this distance the trajectory of a 100 μm diameter pellet is sufficiently reproducible (i.e. within a few milliradians) to permit reliable interception using a 10J, 20ns, ruby laser - giving a fully ionized plasma of maximum ion energy 200ev. Electron-ion recombination is observed experimentally if the plasma is allowed to freely expand to > 15cm, due to the decrease in electron temperature.

Recent developments

To permit reliable interception of the pellet at greater distances (30 - 100cm) from its source, an on-line computer-controlled system has been constructed to steer a Nd glass low beam (having an energy of 100-150J, in 20-60ns) on to the target. The present positional accuracy

of the system is 60-90 μm. The computational and mechanical response of 30ms (each) have proved sufficiently short to permit the reliable interception of xenon ice pellets (170μm diameter, 300μm long). A high repetition rate spherical H_2 pellet injector, multi-beam irradiation (to ensure greater isotropy of the plasma blob), and Nd glass/CO_2 hybrid laser-irradiation schemes are now being considered.

Computer simulation of plasma production

A 1D, two-temperature Lagrangian code is used to compute the D_2 burning and heating phase, assuming both classical and anomalous absorption; refraction and induced scattering are not yet included. A wide range of calculations, including the effects of power variation and prepulse, were reported for both CO_2 and Nd wavelengths. For realistic pulse durations, the energy absorption efficiency was predicted to be typically 25 - 50%; CO_2 lasers appeared to be attractive for such applications.

Other work

Strong plasma assymmetries were experimentally observed when thin glass wire targets (10, 20, 100 or 500 μm dia) were irradiated transverse to a confining magnetic field. Feasibility studies for an intense 14Mev neutron source were also outlined and discussed in detail in Session IX.

(2) I. J. SPALDING (Euratom/UKAEA Fusion Association, Culham Laboratory.)

Dr. Spalding apologized that it had not proved possible to organize talks at the meeting to cover the significant work being undertaken in the U.S.A., and U.S.S.R., in this field. Within Europe, there was a very active interest in laser-filling present-generation toroidal confinement devices, for reasons previously outlined in a Euratom Advisory Group Report on Heating and Injection (EUR. FU.74/AGHI 10/R1; Section B.5(c).) Page 75 of that report tabulates important parameters of seven contemporary European machines, most of which can contain plasma energies of order 1kJ; future requirements will be much greater. For some of these applications the laser has to compete with very efficient alternative heat sources (eg. ohmic heating, or neutral injection). However, laser technology is still progressing very rapidly; already electrical efficiencies of some 60% and 200% have been claimed for CO (long pulse, electrical discharge) and HF (short pulse, chemical) lasers, respectively. For some confinement experiments, it could prove very useful to avoid externally induced plasma currents. Both Garching and Culham were therefore involved in such work (for WIIB and CLEO stellerators respectively) as part of a co-operative Euratom programme. It was hoped

to use a Garching-designed H_2 pellet source on both experiments, but it was not appropriate for him to describe the work of the other laboratories in greater detail.

The Culham experiment would use a 160 litre-atmosphere electron-beam preionized CO_2 laser to provide the main heating pulse, although λ = 1 or 10μm prepulses could also be used if required. The commercial (Systems, Science and Soft ware) cold-cathode electron gun had been successfully operated at energies up to 270kv, and used to preionize the active laser volume of 200 x 20 x 20 cm. The amplifier is at present operated at atmospheric pressure, with a reproducible energy deposition of some 200J/litre at a 120kv sustainer voltage. Optical measurements, and sustainer commissioning at 2 atmospheres (using a 200kv, 62kJ sustainer bank) is currently in hand. The amplification of pulses having a duration between 1 and ~ 100 ns in such an amplifier has been analysed numerically (Armandillo E. and Spalding I.J. - Culham preprint CLM-P423, 1975). Optimization of the energy coupling between the laser and the target requires a detailed understanding of non-linear laser-plasma interactions. Preliminary CO_2 laser-plasma interaction measurements have therefore been made at (vacuum) intensities of up to $\sim 10^{13}$ w/cm^2 (Donaldson et al, Proceedings of 7th European Conference on Controlled Fusion and Plasma Physics, Lausanne, Switzerland, September, 1975); this work included the first direct measurement of a laser-induced density-cavity (or soliton). Such effects could have an important influence on the coupling, as predicted numerically by Estabrook, Valeo and Kruer, among others, and were also related to the spectral shifts in scattered light discussed by Professor Yananaka this morning. In summary, several alternative scenarios for the future could be envisaged, depending on (related) scientific and technological laser developments within the next few years.

IMPLOSION DIAGNOSTICS USING X-RAYS

J.P. Babuel-Peyrissac and G.W. Kuswa

Centre d'Etudes de Limeil, France, and ERDA, Washington DC.

A. X-ray diagnostics at Limeil (J.P. Babuel-Peyrissac)

Implosion experiments at Limeil for 1975 and 1976 will be made with a four-beam neodymium laser, in tetrahedron configuration at a level of 1 KJ, 3 ns, gaussian pulse.

Three kinds of X-rays diagnostics are planned:

1) Pinhole cameras

2) X-ray microscope

3) Radiography method (Absorbix)

Calculations which were made with the assumption that 500 J is a absorbed by a spherical polyethylen target when it is irradiated by the four-beam laser with an energy of 1 KJ, give at an initial diameter of 75 μ and an initial mass of 1.63 μg the following parameters at the hot core:

compression ratio	ρ/ρ_0	15 ÷ 20
temperature	T	200 ÷ 300 eV
life time		60 ps

Using a five-beam of the neodymium laser, synchronized with the main four beams, to hit an aluminium target, we produce an X-ray spectrum. After collimation through the target, and using a monochromator to separate the K-alpha line, the X-ray beam is analyzed by an X-ray streak camera. The conversion rate was studied at Limeil and results show that it is necessary to have around fifty Joules on the aluminium target to obtain ten millijoules of the K-alpha line across the target.

The X-ray streak camera is a Thomson one (TSN 503) with a new photo cathode studied at LEP and Limeil. Presently we use 100 Å of gold on a beryllium foil (10 μ).

Taking into account the yield of the photocathode (5 to 7%) and the contrast of K-alpha line, calculation shows that it is possible to observe the variation of the compression with the time and estimate its value to an order of magnitude.

B. Diagnostics in E-Beam Experiments (G.W. Kuswa)

Pinhole pictures are a major tool used in the inertial confinement program to diagnose pellet compression. A refinement which has been particularly valuable in the e-beam program has been to use a target of material identical to the pellet as a point x-ray source for obtaining the point response function of the camera. The material is hit with a point electron beam source such as a linear electron accelerator operating at the same

voltage used for pellet implosions, and a reference picture is produced. This reference is used in a numerical routine to enhance images of target shots taken with the identical pinhole camera apparatus. In this way vastly improved image information is obtainable. The same technique should be of use in laser implosion work. Microchannel plates have also been useful in x-ray diagnostics to boost the sensitivity of x-ray pin hole cameras and to use in the gated mode for resolving events on the nanosecond time scale. A very high contract ratio camera has been made using two channel plates, one in each end of a 30 cm long solenoidal magnetic field for focusing the electron image. The first channelplate converts the inoident x-ray image to a corresponding electron image. The second channelplates amplifies the electron immage and proprinting focuses it onto a phosphor screen coupled to film. The film end of the camera is shielded from the x-ray event to be diagnosed, the camera is gated by applying pulses to both channelplates. The usual application of the camera is to obtain x-ray shadow images of imploding e-beam pellets at various times after the e-beam is fired. The x-ray source used is a small flash x-ray source of 5 - 1 Mev and ~5 KA with an area of a few mm^2. The camera and the x-ray source are simultanously triggered at the desired interval after the e-beam implosion is initiated.

THE ROLE OF SMALLER EXPERIMENTS IN THE LASER FUSION PROGRAMME

M. Gryzinski

Institute of Nuclear Research, Warsaw

A round table discussion on the role of smaller experiments in the laser and electron fusion programme was held during the meeting. It has been pointed out that a search for finding the most effective way of reaching the final goal should be one of the aims of the meeting. The improvement of exchange of scientists and information, especially between the large and smaller centers, seems to be the most important problem at the moment. The Agency, with the help of a number of scientists from different countries, should take care of it.

There was an opinion expressed that the participation of smaller centers whose main line of interest is not exactly laser and electron beam fusion, should be profitable for both the big fusion program and for these centers. There were listed problems which are important for the laser and electron beam fusion and could be solved in different centers all over the world.

List of problems important to laser and electron-beam fusion:

1. Basic physics

Real equation of state

Nuclear cross sections for energies < 5keV

Stability analysis

High pressure discharges

Discharge physics

Transport properties

"Brand X" laser

Intense X-ray sources

2. Diagnostics

Photoelectric effect (keV range)

Probe beams for high densities ($n > 10^{20}$)

$\frac{dE}{dX}$ measurements in ionized gases

3. Technology

Energy storage

Energy transfer

Laser pumping

Photocathods

CONTRIBUTED PAPERS

LASER INTERACTION WITH PLASMA

J. Mizui, H. Kang, T. Sasaki, K. Yoshida,
T. Tschudi, N. Yamaguchi, T. Yamanaka,
C. Yamanaka

Institute of Laser Engineering, Osaka University

and

Institute of Plasma Physics, Nagoya University

Synopsis

In order to investigate the coupling of laser light and plasma, we have performed the laser bombarding experiments on the hydrogen and deuterium solid targets using a glass laser system "GEKKO-I", with energy of 50 J in nsec pulse. The decrease of the reflectivity has appeared at the laser intensity of one order of magnitude larger than the threshold of the parametric instability. A phase modulation of the reflected light has been found to be due to temporal changes of the refractive index. A second harmonic generation and its red satellites with an isotopic effect have also been observed in the hydrogen and deuterium plasma. These experimental results of the laser interaction with plasma can be explained by a linear conversion of the laser light field into the plasma wave near the cutoff region and its related nonlinear processes in higher laser intensity.

Preliminary compression experiment has been tested using a glass laser system "GEKKO-II" with energy of 250 J in nsec pulse, by the holographic technique.

1. INTRODUCTION

Recently much attention has focused on the laser fusion scheme using high density plasma produced by the implosion. To perform the scientific feasibility experiment on laser fusion, we should resolve the following three subjects: physics of laser interaction with plasma, techniques of high compression of plasma and the development of high power, highly efficient lasers.

The interaction between laser and plasma is one of the most interesting phenomena in laser plasma research.[1-3] In particular, the nonlinear coupling of the collective process in plasma is very important for heating.[4] The parametric process (photon-plasma-photon interaction)[5-7] plays an essential role in the anomalous absorption. This process gives the high energy particles,[4] the decrease of reflectivity of laser light and the red satellites with an isotopic effect in the second harmonic generation.[8]

In the recent scattered light measurements, we have observed a self-phase modulation of the incident laser light. This is caused by a different mechanism to that of the red satellite in the second harmonic. To explain these experimental results, we prosume a linear mode conversion[9,10] of the laser light into the plasma wave in the oblique incidence. The second harmonic[11,12] is produced at the resonance (cutoff) region, while the fundamental light is reflected from the turning (near cut-off) region. In the nonlinear process at the turning region, the spectrum broadening both the red and blue in the reflected light shows the self-phase modulation due to the temporal change of the plasma density caused by the ponderomotive force. But the parametric

process (containing a decay and modulational instability)[13] makes the large amplitude ion wave[14] at the resonance region, when the light intensity is beyond the threshold of instabilities. The ion wave may induce the Brillouin scattering carrying the red shifted satellite in SHG.[12]

As for the preliminary implosion study, a glass laser system "GEKKO-II", energy 250 J in nsec pulse was used. The two beams were irradiated upon various thin targets. The time resolved hologram was taken to check the formation of shock waves in plasma. The interference pattern was constructed after the laser bombardment. The generation source of the x-ray was searched by a pinhole camera. The large glass laser system "GEKKO-IV" are now on construction for the scientific feasibility experiment of laser fusion.

2. EXPERIMENTAL ARRANGEMENT

The laser system "GEKKO-I" was composed of the oscillator and 5 stage amplifier section. The oscillator section had YAG and glass socillators which were selectively used to change the laser light spectral width. They were 6 and 60 Å respectively. The oscillator delivered either the Pockels cell Q-switched pulse or the mode locked pulse train, both of which were tailored by the pulase transmission mode technique. The output energy was 50 J in nsec pulse and the beam divergence was less than 1 mrad.

The main part of the experimental setup is shown in Fig.1. The targets were solid deuterium and hydrogen sticks, the dimension of which was 2 × 2 × 10 mm. The laser beam of 40 mm in diameter was focused onto the target by an aspherical lens of local length 50 mm. The focal spot diameter was

about 50 μm. The image of the target was magnified 10 - 20 times to check the focal condition. The accuracy of the focal adjustment was 25 μm.

The reflected and scattered light spectra were investigated in the range of the incident spectrum and its second harmonic using a Czerny-Turner grating spectrometer with a mean dispersion of 8 Å/mm in first order. The spectrum of the infra-red region was observed using an infra-red vidicon (PbS Photo-surface). The ratio of the incident to the reflected laser light was measured by using a single biplanar photodiode, HTV-R317, with a filter, IR-80.

The electron temeprature was estimated from the soft x-ray measured by plastic syntillators with beryllium windows of different thickness (100, 200, 400, 800 μm).

A glass laser system of "GEKKO-II" (Table I) was used to testify the implosion process by using 2 beams. The target was a thin plastic film of a few 100 μm in thickness and pellet, 20 to 50 μm in diameter levitated in vacuum by CW Ar laser light. Fig.2 shows the experimental arrangement of the time resolved hologram for the shock process in plasma. It can take a series of framing pictures whose time spacing is 100 psec. The double explosure is accomplished for the inteferometric hologram.

3. EXPERIMENTAL RESULTS

3.1 Laser Coupling to Plasma

3.1.1 Reflection of laser beam and plasma heating

The electron temeprature estimated by the foil absorption method[15] of soft x-ray from the plasma is shown in Fig.3. In the glass laser system, the reflectivity increased up to

18 % and began to decrease above the laser intensity of 1.5 $\times 10^{14}$ W/cm^2, which is one order of magnitude larger than the threshold of the parametric instability. The electron temperature had two components above this threshold. The high-energy component increased as $P^{1.2}$, where P is the spatial averaged laser intensity. The low-energy component had a dependence of $P^{0.6}$. The ion velocity had also two components. These results were reported before.[4]

In the case of the YAG laser system, the reflectivity was always slightly higher than that of the glass laser system, and the separation of the high-and low-energy components was not clearly observed.[3]

The neutron measurement has been performed by glass and YAG laser system. Fig.4 shows the relation of neutron yield versus laser energy. The neutron production was assumed to be isotropic for the whole solid angle. It was also checked experimentally using a locating technique that the main source of the neutron was the target itself.[16] To get the same amount of the yield, the YAG laser system needed twice energy of the glass one. The dependence of the neutron yield to laser energy accorded with 5th powers of the energy in the low power and as pointed by the Limeil group[17,18] tended to saturate in the high power.

3.1.2 Scattering spectra of laser beam

We performed measurements of the angular distribution and the spectra of the scattered light around the wavelength of the incident laser, 1.06 μm, and its second harmonics, 5300 Å. Table II summarizes the results for the scattered light at the direction of 0° (backward), 45°, and 90° from

the laser beam. The second harmonic and its satellites on the red side were observed[8,19,20] in all directions when the electric-field vector of the incident laser light was perpendicular to the plane including the wave vector k of the incident laser light and the scattered light. But they were only observed in the backward direction when the electric field direction was in that plane.

The power dependence of the back-scattered second harmonic was found to be proportional to the square of incident laser power with no threshold on laser power. This is due to the linear mode conversion..

Above the threshold laser power of the parametric instability it was accompanied by two side peaks in the red side as shown in Fig.5. These side peaks were especially clear when the YAG laser system was used. They appeared at first in the central part of the laser focus, where the laser intensity reached the threshold of the parametric process. As the laser intensity increased, the intensity of the backscattered light were pronounced and the spatial region of the backscatter source became wide. As for the rate of increase of the side peaks with laser intensity, the glass laser system gave a larger rate than the YAG system did. The frequency shifts of the first peak with the YAG system having the intensity 8×10^{13} W/cm^2 were 84 and 79 cm^{-1} from the center of the second harmonic for hydrogen and deuterium plasmas, respectively. The shifts of the second peaks were 319 and 204 cm^{-1}, respectively. These second peaks showed an isotopic effect. These shifts had no power dependence. In the case of the glass laser

system, the incident spectrum was so broad that the fine structure of the scattered light was smeared.

The spectrum around the second harmonic is not due to scattering excited in the underdense region. These side peaks of the second harmonic seems to be created at the resonance region and are closely related to the parametric instability.

The spectrum of the scattered light around the incident wavelength was affected by the focal position of the laser beam. The backscattered spectrum had two peaks above the laser intensity of 5×10^{13} W/cm^2 when the focal point was in the ranges of 50 $\sim$ 150 μm and 100 $\sim$ 200 μm beneath the surface of the hydrogen and deuterium targets, respectively. One was at the red side of the incident wavelength and anothre was at the blue side as shown in Fig.6(a). However, the backscattered spectrum showed only one peak at the red side of the incident wavelength by 3 $\sim$ 8 Å when the focal point was out of the above-mentioned region or the laser intensity was below 5×10^{13} W/cm^2. And the blue-shifted peak was not observed at the direction of 45° and 90° from the laser beam even at the laser intensity of 10^{14} W/cm^2 as shown in Fig.6(a). The frequency shift of the blue-shifted peak from the center of the incident spectrum was 17 Å for the deuterium plasma at the laser intensity of 1×10^{14} W/cm^2. It increased slightly with the laser intensity, and had no isotopic effect. The onset time of the blue peak was near the time of the maximum of its intensity of the incident pulse whose duration was 3 nsec. The maximum of its intensity appeared after 1.5 nsec from that of the incident pulse. On the other hand, the onset of

the red peak was delayed 1 nsec from that of the incident pulse, and the time of the maximum intensity coincided with that of the incident pulse as shown in Fig.6(b).[24]

3.2 Preliminary Results of Target Compression

Fig.7 indicates the various holograms under different focusing conditions. In Figs.7(a) and 7(b) the laser focus is just on the surface and within the target at the depth of about 200 μm, respectively. We can say that the focal condition is very important to implode the target. From the figure shift of the hologram interferometry the compression ratio was estimated about 3 in solid targets. The x-ray pinhole camera was used to measure the spatial distribution of energetic electron. The energy was 50 keV.

4. DISCUSSION

4.1 Linear Mode Conversion

A second harmonic is generated only when the matching condition, $2k_{\ell}(\omega_{pe}) = k_t(2\omega_o)$ or $k_{\ell}(\omega_{pe}) + k_t(\omega_o) = k_t(2\omega_o)$, are satisfied, where k is wave number, suffix ℓ and t stand for longitudinal and transverse waves respectively, and ω_o and ω_{pe} are the frequency of electromagnetic and electron plasma waves respectively. From our experiments the second harmonic has no threshold or very low one. The laser light is converted to an electron plasma wave under the condition of an oblique incidence. The resonance region is a source of the second harmonic. On the other hand the incident laser light is reflected from the turning region, which is apart from the resonance region. Fig.8 shows the situation of these regions. We assume that the electric-field vector is in the x-z plane.

For a scale length L of plasma inhomogeneity and wavelength λ_o of the electromagnetic wave, there is an optimum angle of incidence θ_o for maximum conversion to a electron plasma wave;[9] $(2\pi L/\lambda_o)^{2/3}\sin^2\theta_o \doteqdot 0.7$. Substituting L = 80 μm and λ_o = 1.06 μm, θ_o is equal to 5°, while the maximum incident angle θ_m is 21.8° in our experiment. As $2\pi\ell_o/\lambda_o$ = 3.9, where ℓ_o is the distance between the resonance region (refractive index N=0) and the turning region ($N = \sin\theta_o$), the distance ℓ_m between the maximum fields of the turning and resonance region is about 1.1 μm. On the other hand the width of resonance region, $\Delta = (\lambda_D^2 \cdot L)^{1/3}$ = 0.16 μm, where λ_D is the Debye length. Because $\ell_m >> \Delta$, we may consider that the SHG and the reflection of incident laser light are independent phenomena, which are shown by our experiments.

4.2 Second Harmonic Generation (Resonance Region)

The mechanism of the geneation of the second harmonic is an interaction between the electromangetic and electron plasma waves in the resonance region. The theoretical predictions[12] have the following characteristic features: (1) The intensity of SHG increases quadratically with the intensity of the incident electromagnetic wave. (2) The electric field vector of SHG is parallel to the x direction. It propagates almost along z direction, and can not propagate parallel to x direction. (3) Above the threshold power of the parametric instability, an ion wave produces the red satellite around SHG. But the blue one is strongly damped. These aspects are closely agreed with our experimental results.

From the theoretical result,[7] temporally growing modes of parametric decay instability into ion-acoustic and electron plasma waves exist in the vicinity of the resonance region across the density gradient, due to the resonance of the pump wave. In order to rise this instability, the rate of trapping the wave energy in the resonance region (cavity) must be faster than that of leaking the energy due to convection. This requirement can be expressed by the inequality,[14] $|E_p|^2/24\pi n T_e > \frac{\lambda_D^2}{|E_p|}\nabla^2|E_p| \approx \left(\frac{\lambda_D}{\Delta}\right)^2$, where E_p is the field of the electron-plasma wave, which is linearly converted from the electromagnetic wave. If $|E_p|^2 \doteqdot |E_o|^2$, where E_o is the field of the electromagnetic wave, the threshold power for the cavity formation is 2.7×10^{13} W/cm^2. We consider that this value is equivalent to the threshold of parametric decay instability as shown in Fig.3.

Now we can explain the spectrum around the second harmonic as follows: Under the threshold the second harmonic is generated with the condition of $2\omega_{pe} \rightarrow 2\omega_o$ or $\omega_{pe} + \omega_o \rightarrow 2\omega_o$, where ω_{pe} is the electron-plasma wave linearly converted from the electromagnetic wave. Above the threshold of the parametric decay instability, $\omega_o \rightarrow \omega'_{pe} + \Omega_s$, where ω'_{pe} and Ω_s are the frequency of electron plasma wave and ion-acoustic wave respectively decided by the decay condition, the red satellite near the second harmonic is additionally generated with the condition of

$$2\omega'_{pe} \longrightarrow 2(\omega_o - \Omega_s),$$

$$\omega_{pe} + \omega'_{pe} \xrightarrow[B.S.]{-\Omega_s} 2(\omega_o - \Omega_s)$$

and

$$\omega_0 + \omega_{pe}' \xrightarrow[B.S.]{-\Omega_s} 2(\omega_0 - \Omega_s),$$

where B.S. is Brillouin scattering process. The frequency of ion-acoustic wave in the parametric decay instability is 3×10^{12} H_z and $\sqrt{2} \times 3 \times 10^{12}$ Hz for deuterium and hydrogen plasma respectively. In Fig.5 the shifts of the second side peaks of deuterium and hydrogen plasma are experimentally 6.11×10^{12} H_z (204 cm^{-1}) and 9.56×10^{12} H_z (319 cm^{-1}), respectively. The value are very close to the above estimated shift $2\Omega_s$.

4.3 Plasma Heating

Under the threshold of the parametric process the laser energy is mainly supplied to electron by inverse bremsstrahlung.[4] The dependence of the electron temperature on the laser power can be estimated by considering the hydrodynamic motion[21] and has been found to be $T_e \propto P^{2/3}$. Our expeirmental results show in Fig.3 that this law holds for the low energy component of electrons. Above the threshold, taking account of the anomalous absorption, the relation $T_e \propto P^{4/3}$ is derived from the hydrodynamic analysis.[22] These results agree with Fig.3.

The decrease in reflectivity, which begins at the laser intensity larger than the threshold of the parametric process, by nearly one order of magnitude, is explained as follows: At the threshold, the spatial region of the instability is restricted in so small area of the focal point that the reflectivity is still mainly determined by the broader area where the laser intensity is weak enough to introduce the classical absorption. As the laser intensity increases, the

anomalous absorption grows spatially to a larger plasma volumn to reduce the reflectivity.

The difference of heating effect between the YAG and the glass system is caused by the spectral width of the incident beam. Nishikawa and co-workers[23] have presented a theoretical treatment of the double resonance of the parametric excitation using two pumps, both being in resonance with the electron plasma oscillation and at the same time their beat frequency being in resonance with the ion-acoustic frequency. According to this theory, two features result: (1) When the beat frequency $\Delta\omega_o$ is tuned to twice the ion-acoustic frequency $2\Omega_s$ and γ_e is the damping rate of the electron plasma wave, the total threshold power for excitation of the ion wave becomes much lower than that of a single pump, and (2) when the first pump intensity is marginal for the decay instability, a very small second pump red shifted by Ω_s can produce the oscillating two stream instability. The glass laser had a spectral width of $\Delta\omega_o \sim 1.6 \times 10^{12}$ Hz (corresponding to $\Delta\lambda_o = 60$ Å), whereas the width of the YAG laser was only 1.2×10^{11} Hz ($\Delta\lambda_o = 6$ Å). In our case of $\gamma_e > \Omega_s$, Ω_s is 3×10^{12} Hz. Consequently, one can expect the glass laser to approximate the conditions for a double resonance much closer than the YAG laser. This line of reasoning also applies to the excitation of the oscillating two stream instability which requires the large pump threshold than the decay instability. Both types of instabilities can be induced more readily with the broadband glass laser. This effective anomalous absorption is shown by the neutron yield in Fig.4.

The mechanism of neutron emission by laser have been discussed in the hydrodynamic approach.[17] When the shock heating is dominant in the overdense region, the number of neutron is proportional to W^5, where W is the laser energy. And if the electron heat wave is dominant, the one is proportional to W^2. In the case of the excess laser power, the most absorbed energy transforms to the electron energy, and the electron heat front preheats the overdense region and breaks the shock formation.[16] This effect is also observed in Fig.4.

4.4 Self-Phase Modulation (Turning Region)

The electromagnetic wave is mainly reflected from the turning region, and the spectrum broadening around the incident wave length could be attributed to the self-phase modulation of the laser light due to temporal changes of the refractive index, which is the function of the density. We presented a time-dependent behavior of the scattered light in one-dimentional simple model. Without absorption and charge saparation, the E.M. wave equation is given by

$$i\frac{\partial E_0^2}{\partial t} + i\frac{\partial}{\partial z}\left(v_g E_0^2\right) = -\frac{4\pi e^2}{m_e \omega_0} n^{(2)} E_0^2 \qquad (1)$$

where $v_g = c^2 k/\omega_0$ is the group velocity which is the function of z, and t and $n^{(2)}$ is the density perturbation of the second-order. The equations of the plasma in uniform temperature are given by

$$\frac{\partial n^{(2)}}{\partial t} + \frac{\partial}{\partial z}\left(n^{(0)} v^{(2)}\right) = 0 \qquad (2)$$

$$m_i n^{(0)} \frac{\partial v^{(2)}}{\partial t} = -\frac{1}{16\pi}\left(\frac{\omega_{pe}}{\omega_0}\right)^2 \frac{\partial}{\partial z}|E_0|^2 - m_i C_s \frac{\partial}{\partial z} n^{(2)} \qquad (3)$$

where $n^{(o)}$ is the density of zeroth-order, $v^{(2)}$ is the velocity perturbation of the second-order and $C_s^2 = T_e/m_i$ is the ion sound velocity.

When the slowly varying amplitude of the E.M. waves is represented by $E_o = A_o e^{i\int \psi dz}$, the real part of eq.(1) gives

$$\gamma = \frac{2\pi e^2}{m_e \omega_0} \frac{n^{(2)}}{v_g} \tag{4}$$

The phase difference between the reflected and incident wave is

$$\int \gamma \, dz = \frac{2\pi e^2}{m_e \omega_0} \left[\int_0^{L-l_0} n^{(2)} \frac{dz}{v_g} + \int_{L-l_0}^{0} n^{(2)} \frac{dz}{v_g} \right] \tag{5}$$

The frequency shift is

$$\Delta\omega_0 = \frac{\partial}{\partial t} \int \gamma \, dz \doteqdot \frac{4\pi e^2}{m_e \omega_0} \frac{L - l_0}{|v_g|} \frac{\partial n^{(2)}}{\partial t} \tag{6}$$

Therefore the density change near the turning region ($v_g/c \doteqdot 0$) mostly contributes to the frequency shift.

Near the turning region, a large negative gradient of the laser intensity, especially in $|E_x|^2$, appears to introduce the decrease of plasma density by eqs.(2) and (3). The spectrum broadening due to the phase modulation at the turning region appears in the red side of the laser light.

For the higher laser intensity, a swelling hump of the laser intensity due to the amplitude modulation becomes so large that a cavity of the plasma density accompanied with humps in front and rear is produced in the underdense region. Then the back-reflected light shows the blue shifted row as

well as the red shifted peak of the intensity as shown in Fig.6(a). When the pulse width of laser is long, a steady state condition gives $n^{(2)} \doteqdot -\left(\frac{\omega_{pe}}{\omega_o}\right)^2 \times \frac{|E_o|^2}{16\pi T_e}$ from eq.(3) and $\Delta\omega_o$ is proportional to $-\partial|E_o|^2/\partial t$. From this reason the temporal response of the blue row in Fig. 6(b) is delayed from the red peak, owing to the slower formation of the density humps in the underdense region. Judging from the dispersion relation $\omega_o^2 = c_s^2 k^2$ in eq.(2) and eq.(3), the ion waves seems to be responsible to form the density humps.

The threshold power for the blue shifted row is estimated as follow. The rate at which E. M. wave is amplified near the turning region must be faster than the rate at which the ion waves propagate over the region. From the eq.(1) this requirement can be expressed by the inequality

$$\frac{1}{E_o^2}\frac{\partial E_o^2}{\partial t} = \frac{\omega_{pe}^2}{\omega_o}\frac{n^{(2)}}{n^{(0)}} > \frac{2\pi}{(\lambda_D^2 L)^{1/3}} C_s \,.$$

As $n^{(2)} \doteqdot -\left(\frac{\omega_{pe}}{\omega_o}\right)^2 \frac{|E_o|^2}{16\pi T_e}$ and $\omega_{pe} \doteqdot \omega_o$,

$$\frac{\omega_o |E_o|^2}{16\pi n^{(0)} T_e} > \frac{2\pi}{(\lambda_D^2 L)^{1/3}} C_s$$

and the threshold power is 4.4×10^{13} W/cm^2. This value agrees the experimental threshold. This effect is small for the second harmonic, because $v_g(2\omega_o)/C \gtrsim 1$ in the turning region (cf. eq.(6)).

The amount of the frequency shift is

$$\Delta\omega_0 \fallingdotseq \frac{4\pi e^2}{m_e \omega_0} \frac{L-l_0}{|v_g|} \frac{|E_0|^2}{16\pi T_e} \frac{1}{\Delta t}$$

$$= \pm 1.8 \times 10^{12} \text{ rad/sec} \quad (9.6\text{Å})$$

where laser power is 1×10^{14} W/cm^2, $v_g/c = 5 \times 10^{-3}$ and $\Delta t = 10^{-9}$ sec. The difference between the two peaks in Fig.6(a) agrees with $2\Delta\omega_0$. In the case of the laser-produced plasma, the medium expands toward the laser beam. Then the whole spectrum of the broadening is shifted about 6 Å to the blue side as a result of the Doppler effect due to the expanding velocity, 1.8×10^7 cm/sec. The overlapping of the frequency broadening due to self-phase modulation and Doppler shift can explain the experimental results.

5. CONCLUSION

The scattered light around the wavelength of the incident laser and its second harmonics was observed experimentally. Because the second harmonic has no threshold, the laser light is linearly converted to a electron plasma wave in a resonance region under the condition of an oblique incidence. The resonance region is a source of the second harmonic. While the incident laser light is reflected from the turning region. The spectrum broadening both the red and blue side of the reflected light shows the self-phase modulation at the turning region. The ion wave caused by the parametric process in the resonance region induces the Brillouin scattering carrying the red shifted satellite in SHG.

The energy of high power laser was anomalously absorbed by the electrons in the resonance region. In the case of the excess laser power the electron heat front breaks the shock formation. In our experiments the efficiency for neutron yield was better at $4 \times 10^{14} W/cm^2$ (15 J) of the broad band glass laser. The optimum condition depends on the hydrodynamic behavior, which is decided by the target dimension and the effective transport coefficient. It will be next problem to search this transport coefficient due to the above mentioned instability.

Acknowldegement

The authors wish to thank Professor K. Nishikawa and Dr. K. Mima for stimulating discussion and Mr. H. Fukushima for his assistance in performing the experiments.

References

1) N.G. Basov, P.G. Kruiukov, S.D. Zakharov, Yu.V. Senatsky and S.V. Tchekalin: IEEE J. Quant. Electron. 4 (1968) 864.

2) F. Floux, D. Congard, L.D. Denoeud, G. Piar, D. Parist, J.L. Bobin, F. Kelobeau and C. Fauquignon: Phys. Rev. A 1 (1970) 821.

3) *Laser Interaction with Matter*, edited by C. Yamanaka and H.J. Schwarz (Japan Society for Promotion of Science, 1973).

4) C. Yamanaka, T. Yamanaka, T. Sasaki, K. Yoshida, M. Waki, and H.B. Kang: Phys. Rev. A 6 (1972) 2335.

5) K. Nishikawa: J. Phys. Soc. Jap. 24 (1968) 916, 1152.

6) A.A. Galeev and R.Z. Sagdeev: Nucl. Fusion, 13 (1973) 603.

7) R.B. White, C.S. Liu and M.N. Rosenbluth: Phys. Rev. Lett., 31 (1973) 520.

8) C. Yamanaka, T. Yamanaka, T. Sasaki, J. Mizui and H.B. Kang: Phys. Rev. Lett. 32 (1974) 1038.

9) V.L. Ginzburg, The Propagation of Electromagnetic Waves in Plasmas; (Pergamon, New York, 1970).

10) D.W. Forslund, J.M. Kindel, K. Lee, E.L. Lindman and R.L. Morse: LASL Report No. LA-UR-74-894 (Univ. California, 1974).

11) N.S. Erokin, S.S. Moiseev and V.V. Mukhin: Nucl. Fusion, 14 (1974) 333.

12) K. Mima: private communication.

13) H. Ikezi, K. Nishikawa and K. Mima: J. Phys. Soc. Jap., 37 (1974) 766.

14) G.J. Morales and Y.C. Lee: UCLA-PPG Report-211 (Univ. California, 1975).

15) M. Waki, T. Yamanaka, H.B. Kang, K. Yoshida and C. Yamanaka: Jap. J. Appl. Phys., 11 (1972) 420.

16) C. Yamanaka, T. Yamanaka and T. Sasaki, in "Laser Interaction and Related Phenomena", Vol.3, edited by H.J. Schwarz (Plenum, New York, 1974) 629.

17) J.L. Bobin: ibid, 465.

18) F. Floux, et al. ibid, Vol.2 (1972).

19) J.L. Bobin, M. Decroisette, B. Meyer and Y. Vittel: Phys. Rev. Lett. 30 (1973) 594.

20) K. Eidmann and R. Sigel: Phys. Rev. Lett. 34 (1975) 799.

21) J.L. Bobin: Phys. Fluids, 14 (1971) 2341.

22) T. Yabe and K. Niu: J. Phys. Soc. Jap., 37 (1974) 1445.

23) D. Arnush, K. Nishikawa, B.D. Fried, C.K. Kennel and A.Y. Wong: Phys. Fluids, 16 (1973) 2270.

24) C. Yamanaka, T. Yamanaka et al.: Phys. Rev. A., 11 (1975) 2138.

Table I High power glass laser "GEKKO-II".

	PREAMP	MAIN AMP					BOOSTER LASER			
		I	II	III	IV	V	DISC-PREAMP	DISC I	II	III
ROD DIMENSION (mm)	φ 5x330 ℓ	φ 20x320 ℓ	φ 20x320 ℓ	φ 30x320 ℓ	φ 30x320 ℓ	φ 40x630 ℓ	φ 60x450 ℓ	45x80x25 t	45x80x25 t	45x80x25 t
Nd_2O_3 (wt %)	3.5	3.5	3.5	3.5	3.5	3.5	1.5	3	3	3
FLASH LAMP	2	4	4	6	6	10	10	10	10	10
MAX PUMP ENERGY (kJ)	10	20	20	30	30	25	100	100	100	100
PUMP ENERGY DENSITY (J/cm^3)	188	212	212	142	142	178	98	108	108	108
INPUT ENERGY (J)	0.002	0.04	0.56	4	7.2	12	50	120		
OUTPUT ENERGY (J)	0.04	0.56	4	7.2	12	50	20	240		
GAIN	7	40 (THREE PASSES)	7	1.8	1.6	4.2	2.4	2		

Table II

Angular dependence of scattered light. Case A is for $\perp E$ (for the incident laser sight) Perpendicular to the plane of $\parallel k$ (for incident and scattered light). Case B is for $\perp E$ in the $\parallel k$ plane.

Frequency		threshold (W/cm^2)	Measurement location		
			Backscatter (0°)	45°	90°
$\omega_o-\Delta\omega$	A	no	yes	yes	yes
	B	no	yes	yes	yes
$\omega_o+\Delta\omega$	A	$(5\sim10)\times10^{13}$	yes	no	no
	B	"	yes	no	no
$2\omega_o$	A	no	yes	yes	yes
	B	no	yes	no	no
$2\omega_o-\Delta\omega$	A	$(2\sim3)\times10^{13}$	yes	yes	yes
	B	"	yes	no	no

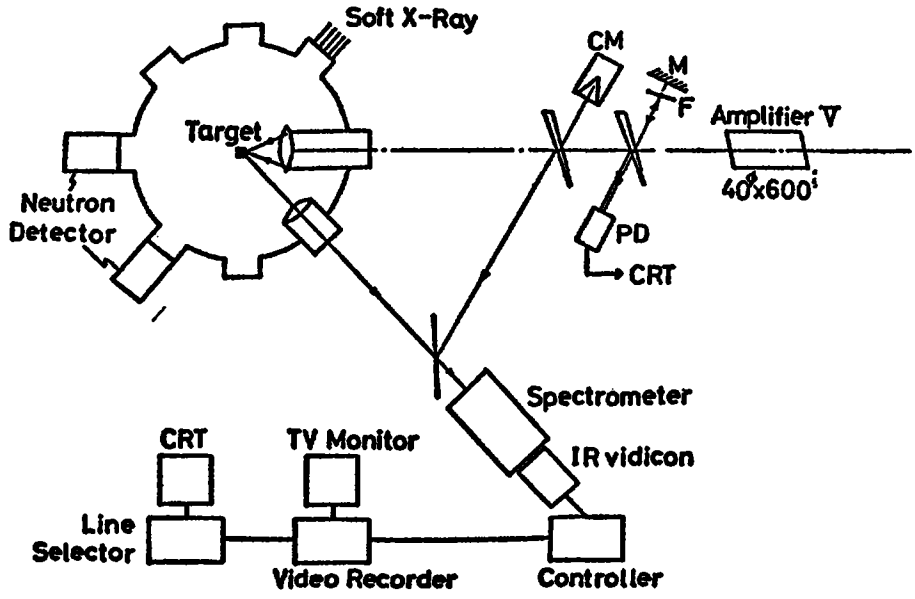

Fig.1 Main part of interaction experiment by Nd glass laser (GEKKO-I).

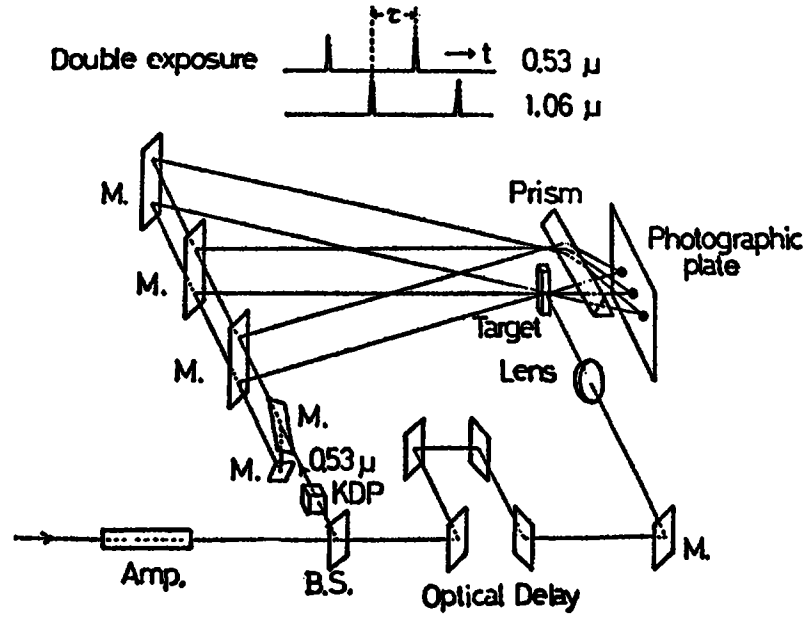

Fig.2 Arrangement for time resolved holography for shock process in plasma using SHG of YAG laser system. Time resolution is 100 psec.

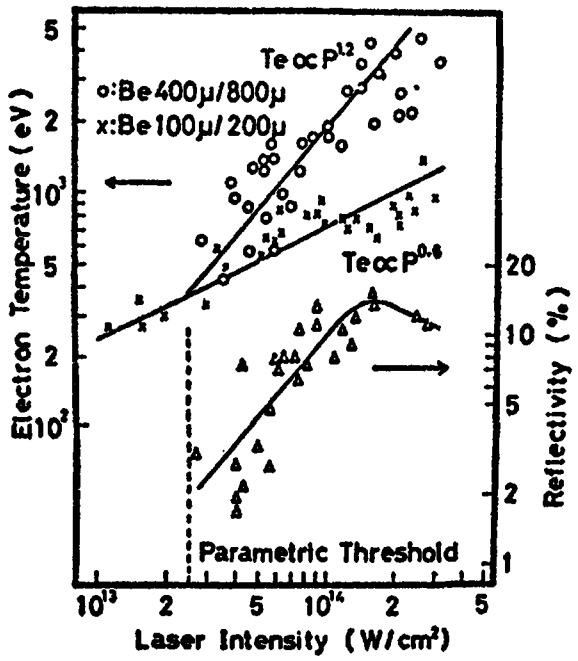

Fig.3 Electron temperature and reflectivity versus laser intensity when glass laser system bombards a solid deuterium target.
Threshold of parametric instability is indicated by vertical line.

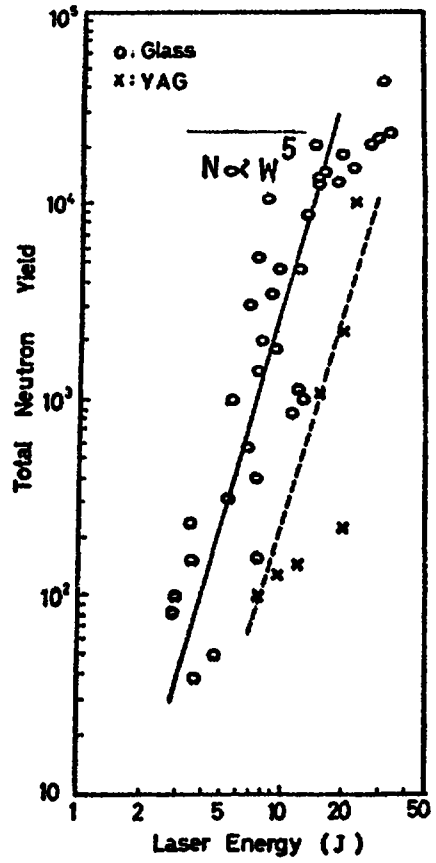

Fig.4 Neutron yield versus laser energy.

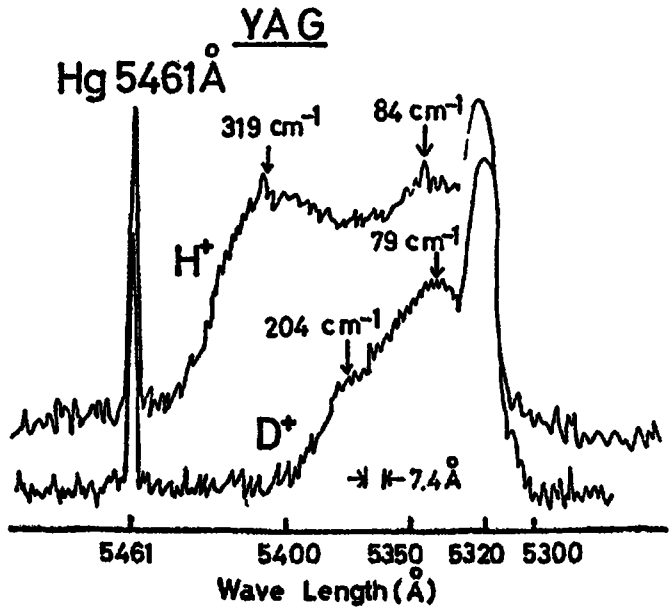

Fig.5 Spectrum of backscattered light near the second harmonics when YAG laser system bombards solid deuterium and hydrogen targets.

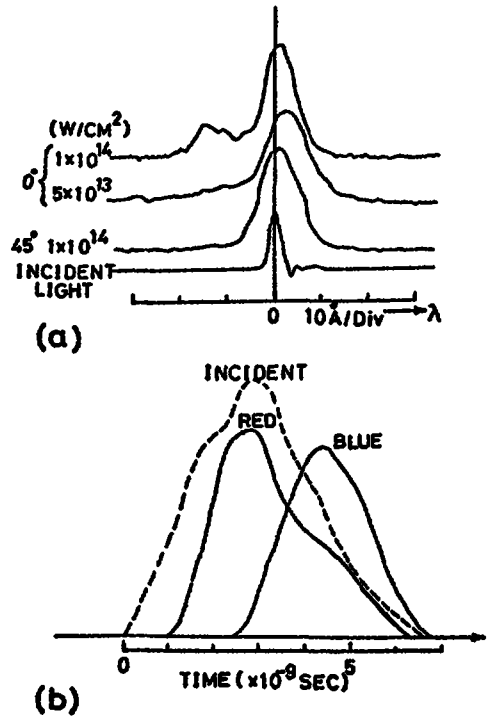

Fig.6 (a) Reflected (0°) and scattered (45°) spectra of incident YAG laser. (b) Time sequence of back-scattered light.

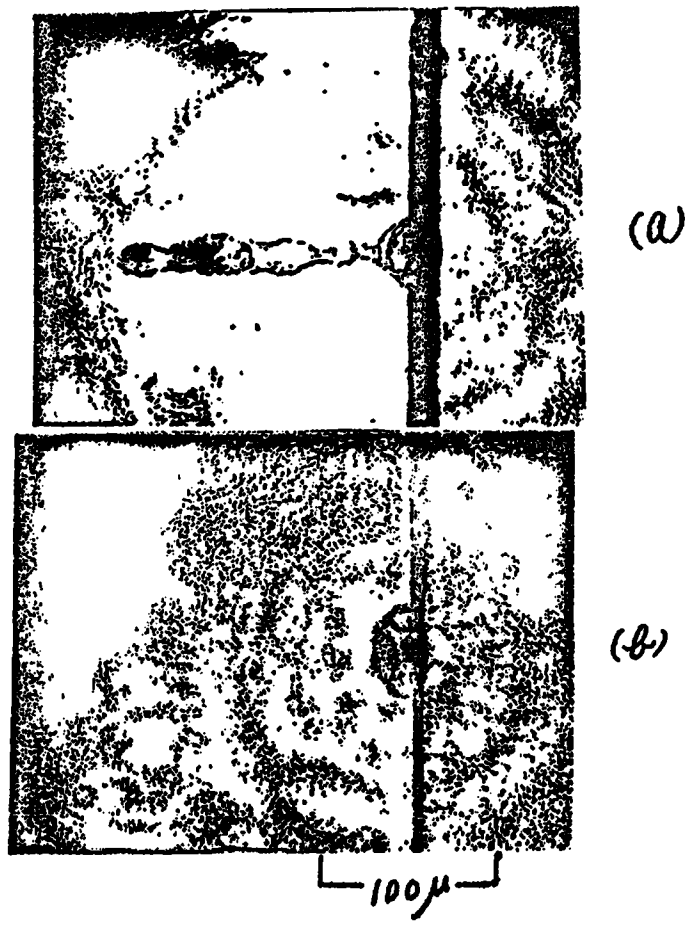

Fig.7 Holographic interferometry

(a) focused just on target surface.

(b) focused within target material at the depth of about 200 μm.

The second harmonic light of the main laser pulse is used for measurement. The pulse duration is 100 psec.

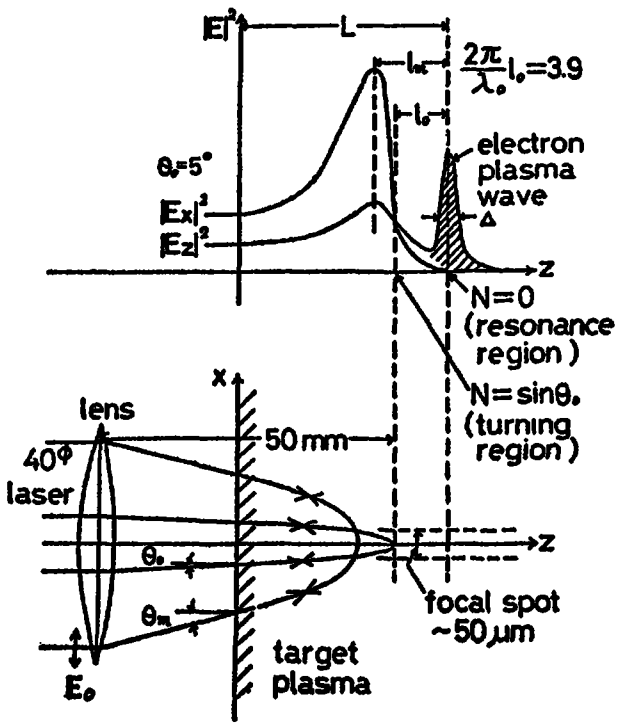

Fig.8 Outline of obliquely incident radiation.

PLASMA HEATING BY INTENSE RELATIVISTIC ELECTRON BEAM

K. Imasaki, S. Nakai, C. Yamanaka

Department of Electrical Engineering, Osaka University

Abstract

Intense relativistic electron beam generators have been constructed for the application of REB fusion research. The electron beam (300keV 40kA) was generated and focused onto the target. The spotsize of the target determined by a 2-channel X-ray pinhole camera is as small as 1 mm. The expanding plasma due to the pinched electron beam on a plain solid target was observed by the streak-camera. From the observation of plasma expanding the heating mechanism of dense plasma by REB seems to be due to the anomaly of the two-stream instability.

1. Introduction

Recently intense relativistic electron beam (REB) has become attractive in the field of research such as pellet fusion[1], plasma heating[2)3)], plasma confinement and heavy ion acceleration. The concept of the pellet fusion by REB is similar to the laser fusion. Comparing with the laser fusion, the main features of REB fusion are as follow, the efficiency of the REB generator ($\sim$ 50%) could be much higher than laser and its total energy ($\sim$MJ) could be much larger. On the other hand, it is difficult to get short pulse of REB ($\sim$ nsec) and fine focusing as laser due to the incoherency and the electric change of the beam. The latter disadvantage (long pulse and poor focusing) could be overcome by using larger pellet corresponding to the possible large energy of REB. The most important problem of REB fusion which must

be investigated is the dissipation mechanism of the beam electron on the surface of the target pellet. The absorption mechanism of REB energy in high density plasma is not so clear as that of laser .

We have investigated focusing of REB, plasma production and heating for the application of pellet fusion. We have constracted three REB generators named REIDEN I, II and III. REIDEN I was to develope fast high voltage technology. With REIDEN-II we have investigated the performance characteristics of REB generator and the interaction mechanism of REB with solid target. REIDEN III is the scale up of II for the fundamental investigation of pellet fusion. In this report, we present the experimental result by REIDEN II.

2. Experimental Apparatus (REIDIN II)

REIDEN II consisted of three main components, a Marx generator for initial energy storage, a coaxial water insulted Blumlein type pulse forming line and a field emission diode with target. The schematic diagram of the system is shown in Fig.1. The stored energy of the Marx generator is transfered to the Blumlein line by pulse charging. The Blumlein line is fired by the water gap at one end to form the voltage pulse across the diode at another end. Intense electron beam is generated by the field emission from cathode connected to the center conductor of the Blumlein line. The Marx generator consists of 8 stage and its stored energy is 2.8KJ at 400KV. The outer conductor of the Blumlein line is 1.7m long with 30cm of diameter. The inner conductor of the line is 1.5m long with 10cm of diameter. The center one is 1.5m long with 4cm of diameter. The storage energy of the

line is 0.6Kjoule when charged voltage is 300KV. The characteristic impedance of the Blumlein line was about 13 Ω. The pulse transmission time of the line was 100nsec. The measured beam pulse length corresponded quite well to the designed value. The inductance of the isolating inductor between Marx generator and Blumlein line is 5μH. This value is large enough to isolate the Blumlein line from Marx generator during the pulse formation.

The typical performance of REIDEN II are as follows

Beam Current	~ 20KA
Beam Voltage	~ 300KV
Pulse Length	~ 100nsec
Energy/Pulse	~ 0.3KJ

3. Result

3-1 Diode impedance

The wave forms of the diode voltage and beam current are shown in Fig.2. The diode voltage is monitored by a low-inductance carbon resistance voltage divider consisted of a potted assembly of 75 x 10Ω, resistors. The beam current is measured by the resister ring consisted of 120 x 10Ω, resistors in the return path. The time resolution of the voltage monitor is less than 10nsec. The resister ring has almost the same time resolution.

From diode voltage and beam current wave form, the variation of the diode impedance is obtained, which is shown by the circles in Fig.3. In this case the brass plain cathode of 30mm in diameter was used with 5mm of separation to brass anode. The pressure at the diode chamber is about 1×10^{-4} torr.

In general the diode impedance can be described by the Child-Langumire relation. In early stage of the pulse the field emission comes from the protrusions on the cathode surface and then rapid vaporization and ionization of the protrusions takes place due to high current density.[4] This cathode plasma works as the virtual electrode. Therefore the diode impedance is decreased from this plasma dynamics. Considering these effect, the impedance of a plane-parallel diode consisting of a disk cathode of radius r and a diode gap d can be given by

$$Z_D = \frac{9}{4\varepsilon_0 \pi}\left(\frac{m}{2e}\right)^{1/2}(d-ut)^2 r^{-2} V^{-1/2} \qquad (1)$$

where V is the voltage across the diode, ε_0 is the dielectric constant in vaccum, m is the mass of electron, e is the charge of election, u is the velocity of expanding plasma from cathode and t is the time after pulse beginning. From equation 1, the theoretical time history of the diode impedance is given as (b) in Fig.3. In this case u is equal to 4×10^6cm/sec which is reasonable velocity of this plasma. The experimental time history of the diode impedance shows a good agreement to equation 1.

3-2. Beam focusing and plasma generation.

REB was focused onto the target using a glass rod 3mm in diameter 10mm long. The configuration of the diode is shown in Fig.5. The electron emitted from the cathode is pinched to the center by the self-magnetic field and is carried to the anode in the plasma generated from the glass rod.

Phenomelogically the emitted electrons move along the glass rod surface[5].

To determine the focusing spot size on the target, 2 channel X-ray pinhole camera utilizing absorbing foils of two different thickness was set. In Fig.4 the densitometer traces of X-ray image along the polyethylene target surface are shown with a 100μm thick Be absorber, (1) and with a 600μ Be one, (2). In Fig.4, the region A corresponds to hard X-ray generation by bremsstrahlung of the beam electron and region B the soft X-ray due to the heated plasma. From this observation the focal spot size of REB on the target was determined as small as 1mm or less. The maximum current density has been estimated to be more than $10^6 A/cm^2$ with corresponding power density of $10^{11} watt/cm^2$.

The intense light generated from the target, when electron beam bombard it, was identified to be the ion lines of C and H of polyethylene. The streak photographs of beam produced plasma were taken with two different orientations of slit. Photograph (a), was along the surface of the target and photograph (b) was along the axis of the electron beam, as shown in Fig.5 The streak photographs in Fig.5 show that the plasma produced by the pinched electron beam expanded only along the target surface. When the target was exchanged with copper the similar behavior of plasma was observed. Therefore observed expansion was not caused by the surface breakdown along the target surface due to charge building up on the insulating anode by the beam electron.[6] Figure 6 shows the expanding velocity of the plasma observed by the streakcamera vs the acceleration voltage of the electron beam.[7]

4. Discussion

There are two possible mechanisms for the energy ransfer of the elecgron beam to the plasma : the collisional dissipation and collective interaction with the plasma. The energy loss of the beam electron by the collision and cerenkov radiation is given by[8)]

$$d_{E/dx}=2\pi r_0^2 n_i mc^2\beta^{-2}[2Z\ell n\ (mc\lambda_0\sqrt{\gamma^{-1}}/2\tilde{h}) + (1/2)Z_i\ell n(\beta mc^2/kT)] \qquad (2)$$

where r_0 is the dassical electron radius, $2\pi h$ is the Planck's constant, n_i is the target density, Z is the atomic number of the target material, Z_i is the change state of the ions, T is the plasma temperature, β is v/c, c is the light velocity, γ is the mass factor and λ_0 is Debye length. Retaining the first term of above equation, the stopping length λ_1 is given by

$$\lambda_1 \propto E_e^2 \qquad (3)$$

where E_e is the beam electron energy. If the total beam energy which is given by child-Langmuir current $\varepsilon_{total} \propto E_e^{5/2}$ is absorbed in the distance λ_1 the plasma temperature T is given by

$$\varepsilon_{total} = sn_1kT\lambda_1 \qquad (4)$$

where s is the cross section of the pinched electron beam, n_1 is the plasma density and k is the Boltzmann constant. Hence the expanding velocity v_p of the plasma due to plasma temperature T is

$$v_p \propto E_e^{1/4} \qquad (5)$$

As for the two stream instability the maximum linear growth rate σ, in the case of cold plasma and cold beam, is

approximately given by $\sigma=0.7(n_2/n_1)^{1/3}\omega_p$ where ω_p is the electron plasma frequency and n_2 is the electron density of the beam[9]. If the instability induces the dissipation of the beam, the decay distance λ_2 is given by

$$\lambda_2 = (v_e/\sigma)\ell n(E_e/E_0) \qquad (6)$$

where v_e is the electron velocity of the beam and E_0 is the thermal energy of the plasma. Substituting λ_2 instead of λ_1 to the eq.(4), the dependence of v_p on the E_e is given by

$$v_p \propto E_e^{7/6} \qquad (7)$$

In Fig.6, the solid line shows the dependence of eq.(7) for the hydrogen of the polyethylene target and broken line is for Cu target. If the two body collision is assumed to be the heating mechanism, the interaction distance λ_1 is one order of magnitude larger than the λ_2. Then the temperature becomes lower than the case of two stream instability.

6. Conclusion

REB generator of moderate size REIDEN II was designed and constructed. By using this machine, interaction of REB with high dense plasma has been investigated. The main results are as follows,

1) Good correspondence of Blumlein performance to designe parameter was asertained.
2) The time history of the diode impedance showed a good agreement with plasma cathode theory.
3) The energy density of the beam was up to 10^{11}watt/cm^2.
4) The stronger interaction beyond the collision theory was observed. The experiment result accorded quite well to the theory of two stream instability.

References

1) F. Winterberg Nuclear Fusion 12 353 (1972)

2) P.A. Miller et al Phys. Rev. Letters30 958 (1973)

3) G.C. Goldenbaum et al Phys. Rev. Letters32 830 (1974)

4) S.E. Graybill IEEE Transaction on Nuclear Science NS-18 438 (1971)

5) D.L. Morrow et al Appl. Phys. Letters 19 441 (1971)

6) K. Imasaki et al J. Phys. Soc. Japan 37 881 (L974)

7) K. Imasaki et al J. Phys. Soc. Japan 38 1554 (1975)

8) G. Yanos et al To be published in Nuclear Fusion :

9) O. Buneman Phys. Rev. 115 503 (1959)

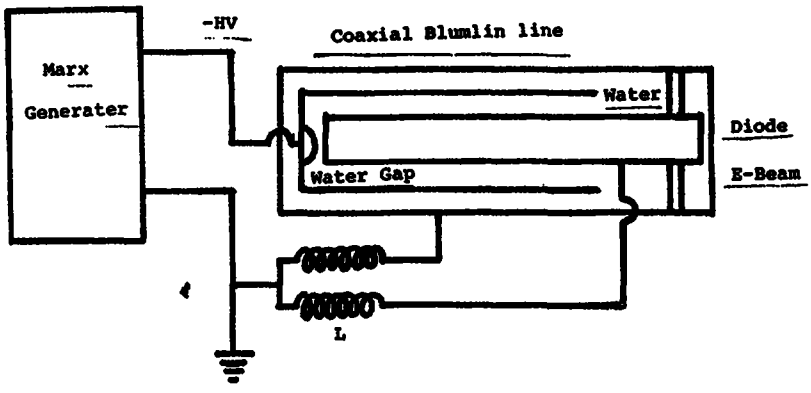

Fig.1 The schematic diagram of the system.

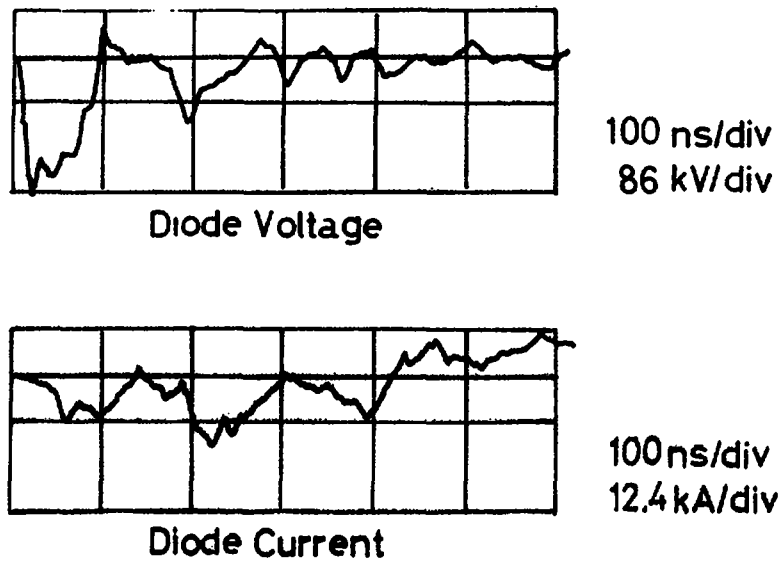

Fig.2 The wave forms of the diode voltage and beam current.

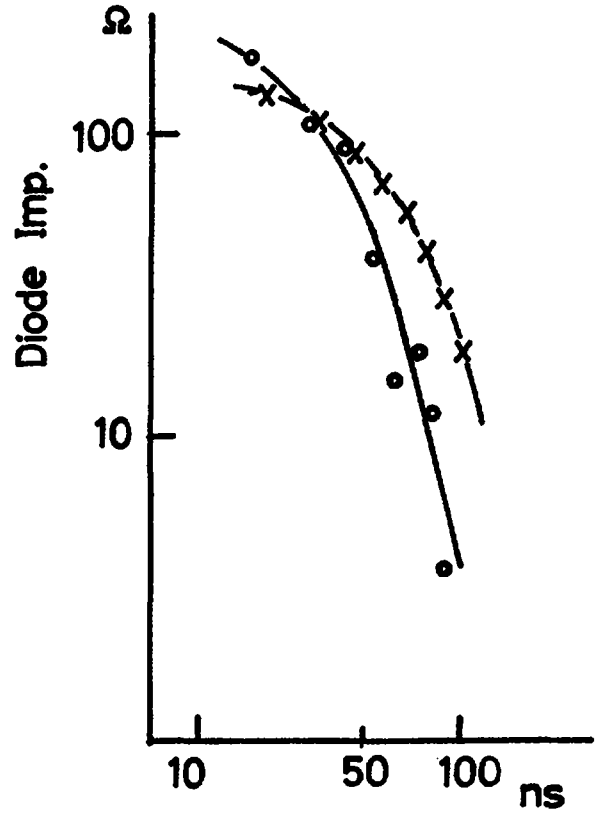

Fig.3 The variation of the diode impedance.

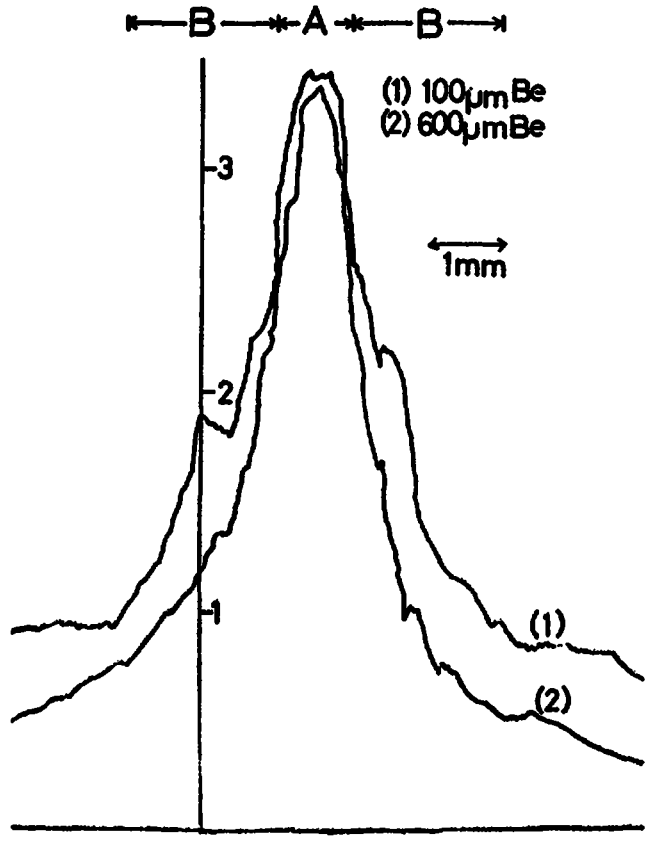

Fig.4 The densitometer traces of X-ray image along the polyethylene target.

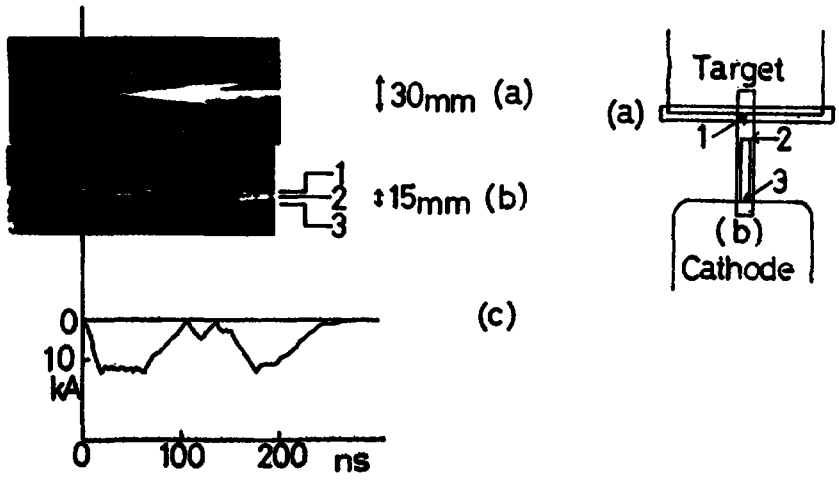

Fig.5 The streak photographs and diode configuration.

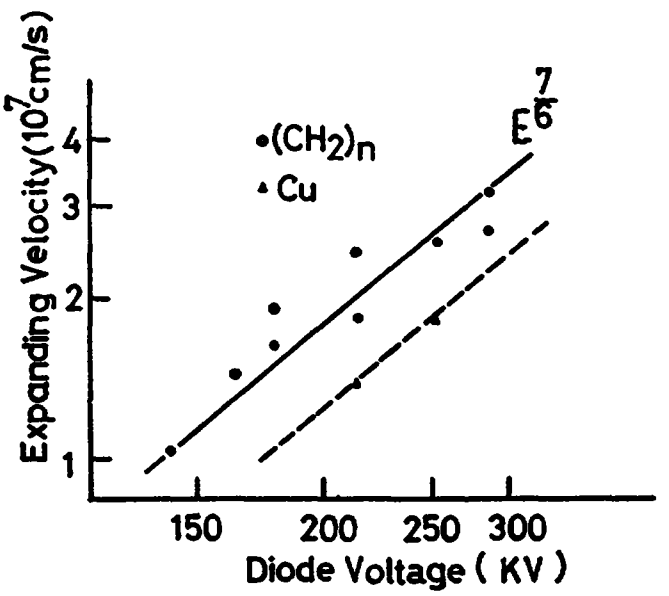

Fig.6 Expanding velocity is observed by the streakcamera.

o the experimental results using polyethylene target.

Δ the experimental results using Cu target.

SOME REACTOR IMPLICATIONS OF LASER (OR RELATIVISTIC BEAM) FUSION

I. Spalding

UKAEA Culham Laboratory

ABSTRACT

The thermal stability of tamped cryogenic DT spherical-shell targets was considered: it was shown that both black-body radiation and the ambient vapour pressure within the inner most wall of an operational reactor could significantly modify the geometry of some types of target during their transit from the exterior to the centre of the reaction chamber. A "check-list" of some inertial-confinement reactor topics meriting examination by the Advisory Group was also suggested.

INTRODUCTION

Some technological implications of the use of homogenous, spherical, pure DT targets for laser-ignited inertially-confined thermonuclear reactor applications have been discussed previously. The fractional mass-loss of such pellets due to sublimation in transit from a cryogenic "pellet factory" to the centre of the reactor vessel can be kept quite small, i.e. $\leq 3\%$, assuming pellet radii of order 10^{-2} - 10^{-1} cm, working temperatures within the reactor vessel of $\lesssim 1000^{\circ}$ K, ambient Li vapour pressures $\lesssim 1$ Torr, and pellet injection velocities between 1 - 10^{3} m/sec.[1] (Note, however, that the effects on pellet trajectory and implosion symmetry of any departure from sphericity during in-transit evaporation of the micro-crystalline target[2] were not considered in Reference 1).

The present paper examines the implications of using spherical, inhomogenous, cryogenic shell targets of the general type discussed in References 3 - 7 in a similar reactor environment. (Such targets pose a less difficult challenge to the laser designer since the laser pulse can rise almost linearly, to a lower peak power[3-5] The lower incident target intensity also alleviates heat-transport problems at the critical surface.) Because of the very wide range of target designs which have been discussed in the literature, the discussion will be restricted to two specific target designs in order to illustrate fundamental principles with a minimum of quantitative numerical detail.

TYPICAL MULTI-SHELL TARGETS

Consider targets categorized as "Type IV" in Reference 5. Thermonuclear fuel is deposited on the inner spherical wall of a high Z shell, having inner and outer radii of R_2 and R_3 respectively. The fuel, having a well-defined inner radius R_1, may be cryogenic DT or a chemical compound such as lithium hydride. Table I summarises characteristic dimensions of two targets, A and B, inferred from the texts of References 5 and 6, respectively.

TABLE I - Typical "Shell" Targets

	TARGET "A"	TARGET "B"
Reference	(5)	(6)
R_3 (μm)	484	1000
$R_3 - R_2$ (μm)	~ 3.4 (High Z)	~ 40 (Pb or Au)
$R_2 - R_1$ (μm)	~ 15.9 (Solid DT)	~ 56 (Solid DT)
Laser Input	100 kJ	1 MJ
Laser Pulse duration (τ_1)	3.5×10^{-9} s (Gaussian FWHM)	10^{-7} s (Triangular)
Thermonuclear O/P	< 10MJ? (See Ref.7)	1000MJ
Reactor Wall Radius	~ 1m	~ 5m
τ_t	~ 3.3ms	~ 16.6ms

As discussed in Reference 1, it seems more convenient to fabricate the pellet outside the heated structure of the reactor, and then to insert it (at high velocity) to the centre of the reaction-chamber. We shall conservatively assume that velocities of order 3×10^3 m/sec are practicable, noting that velocities approaching 10^4 m/sec would imply energies of order 1 ev per particle (i.e. far exceeding the DT binding energy) and a target movement exceeding 3% of its diameter during the time of irradiation (τ_1). The times τ_t listed in Table I thus represent reasonable estimates of the transit times to the centre of reactor chambers having inner (vacuum) wall radii of approximately 1 and 5m, respectively.

EFFECT OF REACTOR ENVIRONMENT ON TARGET

The ambient temperature (θ_R) in the reactor is likely to lie within the range 560 - 1000° K, irrespective of details of the reactor design (eg. lithium blanket or "dry wall" designs). Thus the black-body radiation intensity incident on a cryogenic target is of order $\lesssim 5.7$ w/cm^2. A comparable heat flux will be produced by any vaporized lithium (or other gas) having a pressure (P_{Li}) $\gtrsim 4$ Torr. These are the principle heat loads incident on the target; heating due to tritium β-decay is by comparison completely negligible. What would be the consequence of complete absorption (β = 1) of a 5.7 w/cm^2 heat load on the outer surface of the pellet?

One-dimensional thermal diffusion calculations are adequate for these thin-shell (high aspect ratio) targets, and some characteristic thermal penetration depths are listed in Table II, for typical target materials. Here,

$$\Delta Z = 0.68 \sqrt{\kappa \tau_t} \qquad (1)$$

where κ is the thermal diffusivity of the material.

TABLE II - Approximate thermal penetration depths

MATERIAL	ΔZ	
	τ_t = 3.3ms (Target A)	τ_t = 16.6ms (Target B)
Solid (normal) H_2	400 μm	900 μm
Glass	23 μm	51 μm
Au	900 μm	2000 μm

Comparison of Table II and Table I shows that during a transit time of several milliseconds any temperature rise on the outer surface of the pellet will be rapidly conducted to the interior; indeed, temperature gradients of less than 0.4° C are required to conduct a heat flux of 5.7 w/cm^2 through the shell materials of either Target A or B. The initial temperature rise of the solid DT is thus of order

$$\frac{dT}{dt} = (\beta \sigma \theta^4 + 0.25\, P_{Li} \cdot \bar{c}_{Li}) \left([R_2 - R_1][S_{DT}\rho_{DT}] + [R_3 - R_2][S_Z \rho_Z]\right)^{-1} \qquad (2)$$

where σ is Stephan's constant and S and ρ are the specific heat and density of the respective shell materials. This temperature rise is sufficiently

rapid to melt the DT in either target. Numerical summation of the energy needed to melt solid H_2, raise it to its boiling point and subsequently vaporize the liquid indicates that for either target over 10% of the cryogenic shell will evaporate; comparable numbers could be expected for DT, for which less cryogenic data has been published.

Whether the black-body spectrum is fully absorbed by the pellet will, of course, depend on its detailed design; it is often assumed, for example, that a low Z (and therefore partially-absorbing) outer ablative layer may be used to provide conductive "smoothing" of any non-uniformity of the incident laser pulse. The main purpose of the present note is to stress the significant impact the reactor environment could have on cryogenic target stability and design. As a specific example, Rudakov discussed at this meeting the possibility of a 10^{10} - 10^{11} J thermonuclear output pulse being absorbed in 1 tonne of Li blanket; his duty cycle of one pulse every 10 seconds implies exceptional (and energy-consuming) pumping requirements if the ambient vapour pressure is to be held below 4 Torr.

CONCLUSION

Six questions summarize these and other reactor-related issues, which it would seem profitable to discuss at this Advisory Group.

(1) A thermonuclear gain Q (fusion output/laser input) of 1000 was predicted in Reference 6 for a laser input energy of 1MJ, compared to gains of order 100 discussed in American work [7,8]. The probable magnitude of Q determines the credibility of inertial-confinement approaches to civil power production; what are thought to be the major physics uncertainties in these various calculations?

(2) Apart from the relaxation of the laser-efficiency requirement, what are the benefits of a fission-fusion hybrid?

(3) What is the maximum credible benefit to be derived from a successful nuclear-pumped laser development?

(4) Does direct H_2 or CH_4 fuel production (via 14Mev neutrons), rather than electricity production via a conventional thermal cycle, significantly affect the economics of inertial-confinement?

(5) Can <u>double</u> (high Z shell) cryogenic targets (classified "Type V" in Ref. 5) actually be made with reasonable symmetry, and at realistic cost?

(Note that the gas filled targets discussed by Jonas and others, classification "Type III" of Reference 5, are thermally stable to the reactor environment, but are claimed to require highly-shaped heating pulses for maximum thermonuclear output [6]).

(6) Are cryogenic shell targets credible for high-repetition-rate reactor operation? (If not, what thermonuclear gains are predicted using chemically-bound, higher $\bar{Z}$, thermonuclear fuel?)

REFERENCES

(1) Spalding I.J., "Laser Interaction and Related Plasma Phenomena", Vol. 3B, Ed. H. J. Schwarz & H. Hora, pp 775 (Plasma Press, New York, 1974).

(2) Breuckner K., private communication, 1975.

(3) Breuckner K., Erice Summer School on Fusion Reactors (Sept 1974).

(4) Physics Today, Vol. 28, No. 3, pp17, (March 1975).

(5) Fraley, F. S., et al. Fifth Conference on Plasma Physics and Controlled Thermonuclear Research, Tokio, Japan (1974).
Paper IAEA-CN-33/F5-5 (To be published).

(6) Afanasev Yu. V., et al. JETP Lett 21, 68 (1975).

(7) Clarke J. S., Fisher H. N., and Mason R. J., Phys. Rev. Lett 30, 89 and 249 (1973).

(8) Nuckolls J., et al. Nature (London) 239, 139 (1972).

LASER INDUCED NON-LINEAR PLASMA PHENOMENA (SELF PHASE MODULATION OF LIGHT) AND ANOMALOUS ABSORPTION OF REB IN PLASMA

C. Yamanaka

Osaka University, Institute of Laser Engineering

Abstract

The interaction between laser and plasma, such as mode conversion of laser light to plasma wave, second harmonic generation at the resonance region (cut-off region), red shifted satellites with an isotopic effect in SHG-light and self-phase modulation of back-scattered light from the turning region were discussed.

Also the anomolous absorption of relativistic electron beam in plasma was shown which is interpreted by the two-stream instability.

Laser plasma interaction

The interaction region is divided into two parts. One is the resonance region where the electron plasma wave is trapped in a density well of the plasma. (As shown in Fig. 1). In this region the second harmonic is generated according to the matching condition $2k_l(\omega_{pe}) = k_t(2\omega_0)$ and $K_l(\omega_{pe}) + K_t(\omega_0) = K_t(2\omega_0)$ where k is the wave number, ω is the frequency and l, t stand for longitudinal and transverse waves. As reported before in this case, if the laser intensity is larger than the parametric decay instability threshold the red satellite is observed with the shift of $2\Omega_s$. The plasma of hydrogen and deuterium shows the isotope shift red satellite which is due to the ion acoustic waves. The detailed selection rule was given at the Tokyo Conference [1].

The incident wave is reflected from the turning region due to the oblique resonance. The spectrum of back-reflected light shows the broadening around the incident light. This is due to the self-modulation of laser light by the temporal change of density induced from the ponderamotive force.

With absorption and charge separation electromagnetic wave is given

$$\frac{\partial E_0^2}{\partial t} + i\frac{\partial}{\partial z}(v_g E_0^2) = -\frac{4\pi e^2}{m_e \omega_0} n^{(2)} E_0^2 + \frac{c^2}{\omega_0}\left(E_0 \frac{\partial^2 E_0}{\partial z^2}\right) \quad \cdots (1)$$

where $v_g = \frac{c^2 k}{\omega_0}$, $n^{(2)}$ is the density parturbation of the second order

$$\frac{\partial n^{(2)}}{\partial t} + \frac{\partial}{\partial z}(n^{(0)} v^{(2)}) = 0 \quad \cdots (2)$$

$$m_i n^{(0)} \frac{\partial v^{(2)}}{\partial t} = -\frac{1}{16}\left(\frac{\omega_{pe}}{\omega_0}\right)^2 \frac{\partial}{\partial z}|E_0|^2 - m_i C_s \frac{\partial}{\partial z} n^{(2)} \quad \cdots (3)$$

where $n^{(0)}$ is the density of zeroth-order, $C_s^2 = \frac{T_e}{m_i}$

From $E_0 = A_0 e^{i\int \psi dz}$

$$\psi = \frac{2\pi e^2}{m_e \omega_0} \frac{n^{(2)}}{v_g} \tag{4}$$

$$\int \psi dz = \frac{2\pi e^2}{m_e \omega_0} \left(\int_0^L n^{(2)} \frac{dz}{v_g} + \int_L^0 n^{(2)} \frac{dz}{v_g} \right) \tag{5}$$

$$\Delta\omega_0 = \frac{\partial}{\partial t} \int \psi dz \doteq \frac{4\pi e^2}{m_e \omega_0} \frac{L}{|v_g|} \frac{\partial n^{(2)}}{\partial t} \tag{6}$$

when the laser light is long, a steady density state gives

$$n^{(2)} = -\left(\frac{\omega_{pe}}{\omega_0}\right)^2 \times \frac{|E_0|^2}{16\pi T_e}$$

then $\Delta\omega_0$ is proportional to $-\partial|E|^2/\partial t$

This indicates that the blue shift is delayed from the red shift. The threshold of the self modulation is given by the fact that the wave swelling rate near the turning region is faster than the ion propagation time over this region

$$\frac{\omega_{pe}^2}{\omega_0} \frac{n^{(2)}}{n^{(0)}} > \frac{2\pi}{(\lambda_0^2 L)^{1/3}} C_s$$

This indicates 4.4×10^{13} w/cm^2 as a typical case.

$$\Delta\omega \doteq \frac{4\pi e^2}{m_e \omega_0} \frac{L}{|V_g|} \frac{|E_0|^2}{16\pi T_e} \frac{1}{\Delta t} = 9.6\ \text{Å}$$

where laser power is 1×10^{14}w/cm^2, $v_g/c = 5 \times 10^{-3}$, $\Delta t = 10^{-9}$, $L = 80\mu$ the whole spectrum is shifted about 6 Å to the blue, due to the doppler effect of the plasma expansion (1.8×10^7cm/sec). The experimental results accord with the above prediction.

The ID calculation has been performed to indicate the temporal change of the spectrum broadening. These results show the reasonable behaviour of self modulation.

Anomalous absorption of REB in plasma.

The absorption mechanism of the REB has been investigated. We found the new results due to two-stream instability.

The beam total energy E_{total} is proportional to $E_e^{5/2}$, where E_e is the beam voltage. The classical absorbing distance is

$$\lambda_2 \sim E_e^2$$

when $E_{total} = S n_1 KT \lambda_1$

where n_1 is the plasma density and "s" is the beam cross section.

The plasma expanding velocity is given by

$$V_p \sim E_e^{1/4}$$

as for the two-streem instability, the linear growth rate $\sigma = 0.7 \left(\frac{n_2}{n_1}\right)^{1/3} \omega_p$ where n_2 is the electron density of the beam.

The dissipation length of the beam is

$$\lambda_2 = \left(\frac{V_e}{\sigma}\right) \ln \left(\frac{E_e}{E_o}\right)$$

then

$$V_p \sim E_e^{7/6}$$

This is better corresponding with the experimental data than the classical dissipation length.

References

[1] - C. Yamanaka, M. Yokoyama, S. Nakai, T. Sasaki, K. Yoshida, M. Matoba, C. Yamabe, T. Tschudi
T. Yamanaka, J. Mizui, N. Yamaguchi
K. Nishikawa

in Plasma Physics and Controlled Nuclear Fusion Research (Fifth Conf.Proc. Tokyo 1974) II, IAEA, Vienna (1975), 421

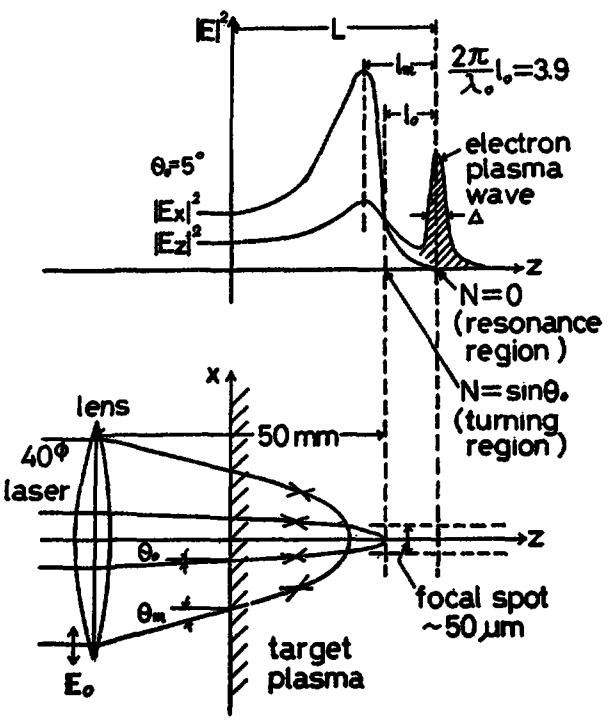

Fig.1 Outline of obliquely incident radiation.

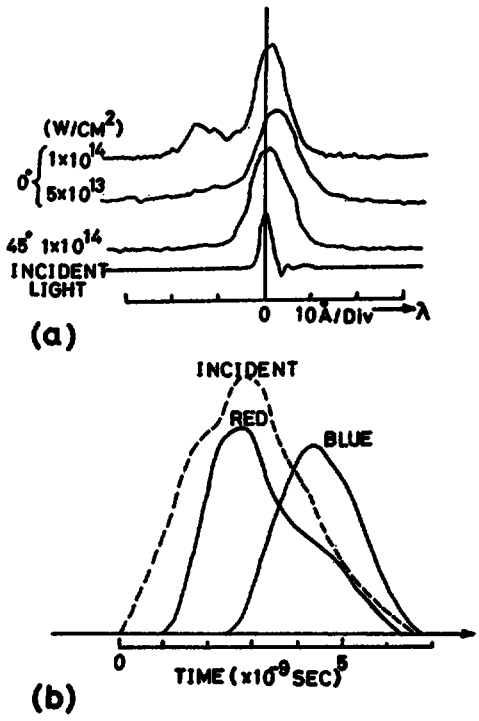

Fig.2 (a) Reflected (0°) and scattered (45°) spectra of incident YAG laser. (b) Time sequence of backscattered light.

ADVISORY GROUP MEETING ON EXPERIMENTAL ASPECTS OF LASER-ELECTRON BEAM PRODUCED THERMONUCLEAR PLASMAS

Trieste, 25-29 August 1975

List of Participants

Country	Name	Affiliation
FRANCE	J.P. Babuel-Peyrissac	CEA Centre d'Etudes de Limeil B.P. No. 27 94 Villeneuve St. Georges
	J.P. Watteau	CEA Centre d'Etudes de Limeil B.P. No. 27 94 Villeneuve St. Georges
	H.J. Doucet	Laboratoire de Physique des Milieux Ionisés Ecole Polytechnique Plateau de Palaiseau 91120 Palaiseau
FRG	E. Fill	Experimentelle Plasmaphysik 4 Max-Planck-Institut f. Plasmaphysik 8046 Garching bei München
	R. Sigel	Experimentelle Plasmaphysik 4 Max-Planck-Institut f. Plasmaphysik 8046 Garching bei München
ITALY	A. Caruso	Laboratori Gas Ionizzati Associazione EURATOM-CNEN Via Enrico Fermi, C.P.N.65 Frascati (Roma)
	S. Solimeno	Istituto Elettroteonico Universita di Napoli Via Claudio, 21 80125 Napoli
	G. Tondello	Istituto de Elettroteonica e di Elettronica Universita di Padova 6/a Via Gradenigo 35100 Padova
JAPAN	A. Mohri	IPP (Institute for Plasma Physics) Nagoya, Japan at present: UKAEA Culham Laboratory Abingdon, Oxfordshire OX14 3DB, UK
	T. Sekiguchi	Dept. of Electrical Engineering University of Tokyo 7-3-1 Hongo, Bunkyo-ku Tokyo 113

	C. Yamanaka	Institute of Laser Engineering (Director) Osaka University Yamada-Kami, Suita Osaka
	T. Yamanaka	Institute of Plasma Physics Nagoya University Nagoya
NETHERLANDS	W.J. Witteman	Technical University Twente Department of Applied Physics P.O.Box 217 Enschede
POLAND	M. Gryzinski	Institute of Nuclear Research Warsaw
SWITZERLAND	K. Appert	Centre de Recherches en physique des plasmas l'Ecole Polytechnique fédéreale 21 avenue des Bains CH-1007 Lausanne
	H. Weber	Institut für Angewandte Physik Universität Bern Sidlerstr. 5 3000 Bern
UK	I.J. Spalding	UKAEA Culham Laboratory Abingdon, Oxfordshire OX14 3DB
	C. Whitehead	UKAEA, B.7.21 AERE Harwell Didcot, Oxfordshire OX11 ORA
USA	G. Kuswa	ERDA Washington DC 20545
	M. Lubin	University of Rochester Rochester, N.Y. 14627
	G. McCall	LASL P.O.Box 1663 Los Alamos, N.M. 87544
	G. Yonas	Sandia Laboratories P.O.Box 5800 Albuquerque, N.M. 87115
	M. N. Rosenbluth (Observer)	Institute for Advanced Study Princeton, NJ 08540
	R. A. Shanny (Observer)	Naval Research Lab., Code 770 Washington DC 20375

USSR	V.A. Gribkov	P.N. Lebedev Institute of Physics USSR Academy of Sciences Leninskii prospekt 53 Moscow V-312
	L.I. Rudakov	I.V. Kurchatov Institute of Atomic Energy 46 Ulitsa Kurchatova, P.O.Box 3402 Moscow D-182
	V.P. Silin	P.N. Lebedev Institute of Physics USSR Academy of Scienoes Leninskii prospekt 53 Moscow V-312
ICTP Trieste	P. Budini	Deputy Director
	A. Hamende	
IAEA Vienna	A.N. Belozerov	Scientific Secretary